



DEGREE PROJECT IN THE FIELD OF TECHNOLOGY  
TECHNOLOGY AND LEARNING  
AND THE MAIN FIELD OF STUDY  
MATHEMATICS,  
SECOND CYCLE, 60 CREDITS  
*STOCKHOLM, SWEDEN 2020*

# **A Spatially Explicit Agent-Based Model of Human-Resource Interaction on Easter Island**

**PETER STEIGLECHNER**

KTH ROYAL INSTITUTE OF TECHNOLOGY  
SCHOOL OF ENGINEERING SCIENCES



# **A Spatially Explicit Agent-Based Model of Human-Resource Interaction on Easter Island**

PETER STEIGLECHNER

Master in Computer Simulations in Science and Engineering

Date: June 13, 2020

Supervisor: Agostino Merico

Examiner: Michael Hanke

School of Engineering Sciences

Host company: Leibniz Centre for Tropical Marine Research (ZMT)

Swedish title: det är en svenska titlen



## Abstract

The history of Easter Island, with its cultural and ecological mysteries, has attracted the interests of archaeologists, anthropologists, ecologists, and economists alike. Despite the great scientific efforts, uncertainties in the available archaeological and palynological data leave a number of critical issues unsolved and open to debate. The maximum size reached by the human population before the arrival of Europeans and the temporal dynamics of deforestation are some of the aspects still fraught with controversies. By providing a quantitative workbench for testing hypotheses and scenarios, mathematical models are a valuable complement to the observational-based approaches generally used to reconstruct the history of the island. Previous modelling studies, however, have shown a number of shortcomings in the case of Easter Island, especially when they take no account of the stochastic nature of population growth in a temporally and spatially varying environment. Here, I present a new stochastic, Agent-Based Model characterised by (1) realistic physical geography of the island and other environmental constraints (2) individual agent decision-making processes, (3) non-ergodicity of agent behaviour and environment, and (4) randomised agent-environment interactions. I use the model and the best available data to determine plausible spatial and temporal patterns of deforestation and other socioecological features of Easter Island prior to the European contact. I further identify some non-trivial connections between microscopic decisions or constraints (like local confinement of agents' actions or their adaptation strategy to environmental degradation) and macroscopic behaviour of the system that can not easily be neglected in a discussion about the history of Easter Island before European contact.

# Contents

<b>1</b>	<b>Introduction</b>	<b>1</b>
<b>2</b>	<b>Mathematical Theory</b>	<b>7</b>
2.1	Differential Equation Based Approaches for Easter Island . . . . .	7
2.2	Agent-Based Modelling (ABM) of Human-Resource Interactions – Overview, Motivation and Previous Approaches . . . . .	10
<b>3</b>	<b>Development of an Agent-Based Model for Easter Island of Human Resource Interaction</b>	<b>13</b>
3.1	Model Overview . . . . .	13
3.2	A Discretised Map of Easter Island with Geographical and Biological Features . . . . .	16
3.3	Human Agents and their Features . . . . .	22
3.4	Agent-Environment Interaction . . . . .	26
3.5	Population Growth . . . . .	29
3.6	Movement of agents . . . . .	33
<b>4</b>	<b>Results and Discussion</b>	<b>47</b>
4.1	A Standard Configuration Run . . . . .	47
4.2	Experiments and Sensitivity Analysis . . . . .	55
4.2.1	Abundance of and Requirements for Resources . . . . .	55
4.2.2	Resource Search Radii . . . . .	57
4.2.3	Population Growth . . . . .	59
4.2.4	Tree Preference . . . . .	60
4.2.5	Moving Strategy . . . . .	62
<b>5</b>	<b>Conclusions</b>	<b>67</b>
	<b>Bibliography</b>	<b>70</b>

<b>A More Details of the Model</b>	<b>74</b>
<b>B More Results</b>	<b>75</b>
B.1 Additional Results: Standard Run . . . . .	75
B.2 Clustering the Agents . . . . .	76
B.3 Additional Results: Variation in the Agents' Strategy of Adapting the Tree Preference . . . . .	77



# Chapter 1

## Introduction

**Population Growth and the Malthusian Theory.** Over the last century, human activity has become a key driver of not only local but also global environmental change. Given the limited resources of our planet, a global population growth from less than 2 to current 7.8 billion individuals within a century raises serious concerns. One of the first theories suggesting a scenario of overshooting population was developed by Malthus (1798). He suggested that, as population size increases exponentially, resources such as fertile land exhaust, leading to increased prices, conflict and the general potential of a collapse of the human society. Later and with a main focus on environmental degradation, the Club of Rome followed this rationale in their report on ‘The Limits of Growth’ (Meadows et al., 1972). Of course, so far no global overshoot has occurred throughout history. It is now more commonly accepted that a global population follows (at maximum) a logistic rather than an exponential growth (e.g. in KC and Lutz, 2017, Figure 1)<sup>1</sup>. Furthermore, technological advances, such as nitrogen fertilisation, have greatly enhanced the access to necessary resources for humanity. Today, however, the awareness about climate change as a real and imminent threat to the planet fuels interest in the Malthusian theory anew (Reuveny, 2012). Hence, it is important to investigate the potential implications for the human society of scenarios of population overshoot.

**Examples of Overpopulation and Resource Exploitation in Ancient Civilisations.** Interesting case studies of potential overpopulation often in connection to environmental degradation are provided by the disappearance of relatively small, ancient civilisations, such as the Maya in Meso-America, the

---

<sup>1</sup>However, this does not necessarily mean that resource and energy consumption also do not grow exponentially.

Anasazi in the South West of the United States, or the Norse in Greenland (Diamond, 2011). In particular, the fate of the Easter Island civilisation, the ‘Rapa Nui’, has captured scientific and public interest for centuries. One reason is the total isolation of the island for several centuries (see Figure 1.1). This provides an ideal, natural laboratory of a socio-ecological system in transformation. Another reason is the substantial environmental change detected on the island following human settlement. Within a relatively short period of time, the initial dense palm tree forest turned into barren land deprived of any large vegetation as observed by the first European voyagers in the 18th century. Finally and most importantly, the platforms (‘Ahu’) and hundreds of statues (‘Moai’) carved, transported to and erected in various places on the island indicate a large population with rich culture, advanced technological know-how, well established political institutions and a working trading economic system (Cauwe and Latsanopoulos, 2011). This impression is in stark contrast to the observed deforested island, with a relatively small and potentially even rivalrous civilisation reported especially in later visits to the island after 1770 A.D.. Resolving this mystery behind the Rapa Nui before European contact has arguably become one of the most intriguing questions in archaeology.

**Facts about Easter Island History.** Numerous studies in the fields of archaeology and anthropology have tried to reconstruct the history of the island and its people before European contact. However, data is often sparse and can be interpreted in various ways (Merico, 2017). For example, many Moai have been toppled in the 18th century which was interpreted as a sign of violence (Bahn and Flenley, 2017) or a religious/cultural burial process (Cauwe and Latsanopoulos, 2011). Often theories on the population dynamics are based on palynological data, i.e. pollen records from sediments in the three crater lakes and charcoal data from excavations. However, there are substantial uncertainties in the dating of such data due to the process of sedimentation including geological gaps and drought periods (Hunt, 2007; Bahn and Flenley, 2017), in the extrapolation to an island-wide data record (Rull, 2020) and, most importantly, in the interpretation of these proxies for human activity and, thus, population dynamics (e.g. Cole and Flenley, 2008). While many aspects of Easter Island history are debated, there are a few typically commonly accepted facts. The relevant ones for this thesis include:

- Before human settlement, the island was forested (Mieth and Bork, 2015; Rull et al., 2010).

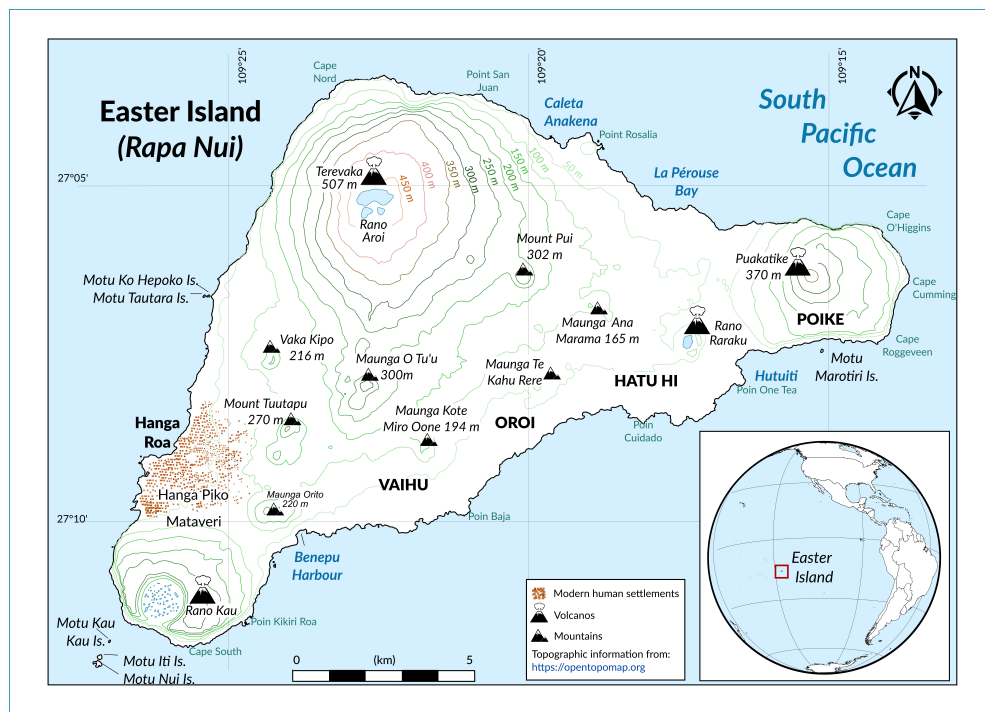


Figure 1.1: Map of Easter Island today and its location in the Pacific taken from Merico (2017). Map courtesy of Jailson Fulgencio de Moura.

- Polynesian rats, which were introduced to the island by the first settlers as a protein source, quickly reproduced and effectively hindered the regeneration of palm forests by feeding on the seeds of the palm trees, thus potentially reducing or even preventing tree regrowth (Hunt, 2007 and Bahn and Flenley, 2017).
- Starting from around 1200 A.D., there is evidence for intensified deforestation in some places on the island (Rull, 2020) but with unknown contributions from different drivers (rats, climate or humans).
- The Rapa Nui farmed land and cultivated sweet potato, taro, yam, and many other crops. They used advanced methods, like lithic mulching, to increase yields (e.g. Louwagie, Stevenson, and Langohr, 2006). However, the fertility of the soil and the climatic conditions for farming remain open questions (Bahn and Flenley, 2017).
- The Moai were carved from the 13th to 17th century, followed by a societal change in the 17th or 18th century (Cauwe and Latsanopoulos, 2011).
- European voyagers arrived in 1722 A.D. and more frequently after 1770 A.D.. They found a (nearly) treeless island and vaguely estimated the population size to be ‘thousands’ in 1722 A.D., between 1000 and 3000 in the late 18th century and only 111 in 1872 A.D. following devastating slave trade and a smallpox epidemic brought by Europeans (Bahn and Flenley, 2017).

### Main Uncertainties and Different Narratives of Easter Island History.

The uncertainties in the dynamics of deforestation and population size have lead to two major, contrasting narratives about the natural and anthropogenic contributions to deforestation, the correlated population dynamics and, therefore, the overall sustainability of the Easter Island civilisation. On the one hand, a ‘genocidal’ view (Hunt, 2007), on the other hand, an ‘ecocidal’ view (Diamond, 2011; Bahn and Flenley, 2017). According to the genocidal view, the first settlers arrived around 1200 A.D., the population size quickly grew to a plateau of 4000 individuals and remained at this level for several centuries. Deforestation is attributed not only to human activity but was crucially fostered by the fast expansion of the Polynesian rats. However, the human society remained mostly resilient to this environmental degradation only to eventually be diminished by the introduction of European diseases and slave

trade. According to the ecocidal view, the arrival of the first settlers occurred before 1000 A.D.. The population then grew steadily and burnt trees to clear land for agriculture. This development intensified around 1200 A.D.. Population size peaked some time after 1500 A.D. at levels estimated between 6000 to 8000 or 10000 to 20000 (Bahn and Flenley, 2017), followed by a steep decline or even ‘collapse’ (Diamond, 2011) before European contact. The narrative concludes that the Easter Island population overexploited the natural resources and, consequently, got locked in the Malthusian catastrophe of resource shortage, cultural disruption, conflict and consequent population decrease. Next to these two major themes, various other theories have been put forward. E.g. Brandt and Merico (2015) suggest with modelling work (described more in Chapter 2) that a scenario of quick population growth followed by a slow-demise is most consistent with data of charcoal remains. A model developed by Cole and Flenley (2008) suggests the possibility of multiple periods of growth and collapse throughout Easter Island history. The authors used a far-from-equilibrium approach in their population model. However they do not state reasons or drivers for the suggested periods of population decline. Furthermore, Rull et al. (2016) reviews evidence for climatological rather than anthropogenic drivers of deforestation, arguing for a more holistic perspective. All of these contrasting narratives, ultimately, are not based on direct evidence for population sizes but rely on uncertain proxy data. Therefore, interpretations and, thus, assumptions vary strongly and might be ‘spectacularly ill-posed’ (Merico, 2017) if new evidence is discovered. The dynamics of population size and deforestation and its causes remain a fiercely debated topic as the different narratives strongly correlate with personal perceptions of the Rapa Nui and their response to an environmental crisis.

**Mathematical Modelling of Socio-Economic Systems of Ancient Societies.** Easter Island history has been studied in various disciplines, from archaeologists to anthropologists. A major contribution, however, has been made by socio-economic modelling. Mathematical modelling, typically with macroscopic system models, has provided a workbench for testing hypotheses and scenarios of natural and anthropogenic dynamics on Easter Island given a certain set of assumptions. I describe these models and the shortcomings they share in Chapter 2. In this thesis, I take a different approach that is based on Agent-Based Modelling (ABM). Such a new model can help to understand the complexity of the socio-ecological microcosm of the island by focusing on individual behaviour, uncertainty and spatial constraints rather than simply adding another macroscopic theory to the research body with assumptions

based on insufficient data.

**Outline** In Chapter 2, I describe both types of mathematical models, the various existing macroscopic system models and the approach of Agent-Based Modelling considered in this thesis. In Chapter 3, I develop such an Agent-Based Model from scratch by defining a spatially explicit environment, human agents with specific features and their various actions and interactions. I also justify the choices and assumptions made in this model with conclusions or data from the existing literature and plausible arguments, when data is not available. In Chapter 4, I then present some of the results obtained with this model and discuss the implications of different choices of assumptions and parameter values on the spatial and temporal dynamics produced by the model.

# Chapter 2

## Mathematical Theory

### 2.1 Differential Equation Based Approaches for Easter Island

**The Basic Ordinary Differential Equation Model.** Theories on the population dynamics and deforestation on Easter Island are typically supported by a mathematical, human-resource interaction model. So far, all these models are based on aggregate predator-prey type of interaction between humans and resources (so called Lotka-Volterra model). The dynamics of these macroscopic variables is then described by non-linear, coupled ordinary differential equations (ODEs). The first and most famous model was developed by Brander and Taylor (1998). The authors simulate the dynamics of two variables, a growing human population  $L$  (the predator) and a logistically growing, open-access resource with stock  $S$  (the prey). This resource can be interpreted as the forest/soil complex, which is slowly renewable in this model. Of course, the Rapa Nui did not live off trees but they provided valuable derivate products or ecosystem services e.g. as habitat for birds, firewood, wood for tools or the transport of the Moai statues, or even for extracting a sugary sap as a supplement for freshwater (Bahn and Flenley, 2017). Palm forest is, thus, often considered as the primary resource in Easter Island models. Consumption of the resource by humans enables population growth. Hence, the human population harvests  $H(L, S)$  from the resource, and thereby depletes its stock. The system is described by the set of ODEs

$$\frac{dL}{dt} = L \cdot (b - d) + \phi \cdot H(L, S) \quad (2.1)$$

$$\frac{dS}{dt} = G(S) \cdot S - H(L, S), \quad (2.2)$$

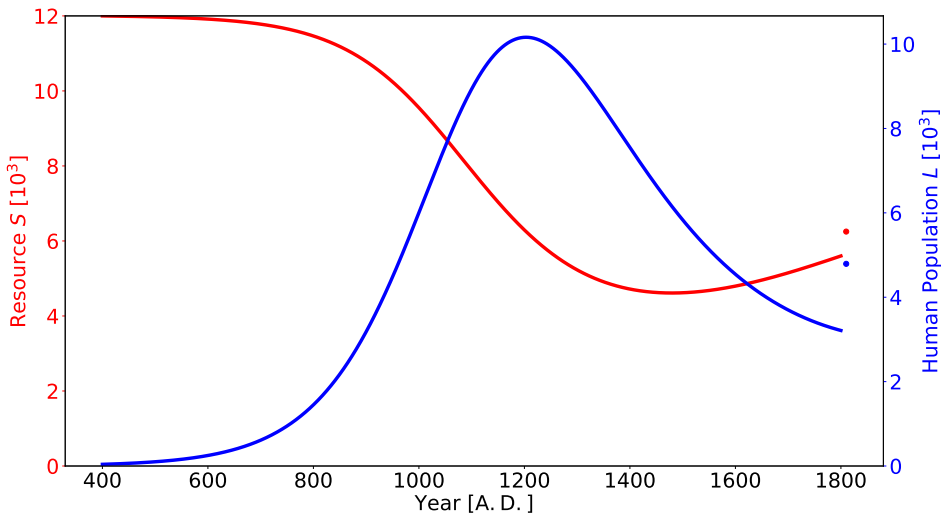


Figure 2.1: Replication of the model in Brander and Taylor (1998) with parameter setting as in the ‘Easter Island Base Case’ in Figure 3 of the publication. The dots on the right represent the equilibrium values.

where  $b$  and  $d$  are, respectively, constant birth and death rates of the human population,  $\phi$  denotes the increase of fertility with resource consumption and  $G(S)$  is the logistic growth rate of the resource. This model applied to Easter Island reproduced a ‘boom and bust’ cycle (Figure 2.1), which, as the authors argue, is an example of the ‘Malthusian forces [leading] to a depletion of the resource base and social conflict’ and, thereby, supports the ecocidal view of Easter Island history.

**Extensions of the Basic Model.** In the last two decades several extensions and adjustments have been added to the first mathematical model by Brander and Taylor (1998). Reuveny (2012) provided an extensive overview of these models. Merico (2017) additionally summarised gaps and advances within this field of research. Here, I point out those models relevant to the word of this thesis. D’Alessandro (2007) separated the single resource into two, one that is inexhaustible and another that is renewable (and irreversibly exhausts if below a certain threshold). The author found multiple stable states due to this disaggregation of the ecological variable. A model by Good and Reuveny (2006) introduced foresight and resource management institutions (either a system of property rights or a social planner). Here, the society’s harvest rate is determined by maximising a utility function over a certain time horizon with reasonable discounting (e.g. by a social planner, which could be an emergent

political hierarchy). However, the authors found that even with optimal institutions in place, a collapse of the Rapa Nui population is inevitable. Basener et al. (2008) added another variable to the model next to tree number and human population size, which accounts for the rat population and their devastating impact on tree regrowth as previously found by Hunt (2007). This model was then further extended by a spatial component (Basener et al., 2011). A number of homogeneous, one-dimensional cells was defined and diffusion of rats and humans allowed between adjacent cells. The authors found that simply changing the mobility of rats can qualitatively alter the dynamics of the human population size. While this representation is extremely simplified and the diffusion process is unintuitive for human settlement pattern of a small island, this is the only model on Easter Island including a physical space. Finally, in a recent analysis, Brandt and Merico (2015) extended the model of trees, rats, and humans by Basener et al. (2008) with a disease spreading model. They found that the model can obtain any of the proposed narratives (ecocide, genocide or the slow-demise) through variation of only a few parameters in a reasonable range. All these models build on the assumptions considered in the macroscopic ODE model by Brander and Taylor (1998).

**Shortcomings of Macroscopic ODE Models.** Despite the extensive body of research presented by the numerous macroscopic system models on Easter Island, the dispute between different narratives could not be solved. The ODE based models, the main tool for Easter Island modelling, typically either showed the same (inherent) boom and bust cycle or showed shortcomings in that different choices of parametrisation (within the uncertainties of the sparse archaeological data) consistently produced contrasting results (Merico, 2017). Next to the uncertainties in the available data to support the assumptions, many shortcomings of these models are inherent problems of macroscopic system modelling. This includes in particular the missing spatial, microscopic constraints, heterogeneity in the human population, the stochastic nature of the spatial and temporal environment, co-evolving behaviour and emergent phenomena. A microscopic, agent-based model addresses many of these issues and, therefore, constitutes a useful alternative to macroscopic ODE model approaches as described in the next Section.

## 2.2 Agent-Based Modelling (ABM) of Human-Resource Interactions – Overview, Motivation and Previous Approaches

**Overview of ABM.** Agent-Based Modelling (ABM) is now a common tool at the centre between cognitive psychology, game theory, and complexity science (Bousquet and Le Page, 2004) with roots in the field of Artificial Intelligence. In Agent-Based Models (ABMs) a system is grown bottom-up from its constituent units. Hence, an ABM focuses on the microscopic rather than the macroscopic aspects of a system. The model simulates a number of discrete agents (e.g. humans), often situated in an environment, with specific traits. Agents (and the environment) are updated asynchronously at certain time steps over the simulated period. In each update, a single agent interacts with the environment and other agents according to a set of rules or heuristics. These rules are usually heterogeneous, non-linear (e.g. discontinuous or discrete), stochastic, time-dependent and adaptive and might be memory- and path-dependent (Bonabeau, 2002). In the case of a spatial model, rules and behaviour additionally depend on the explicit location of an agent in the environment. Usually, agents make individual decisions, based on perceptions of their local surroundings and their internal state, and thereafter act independently and autonomously. With this microscopic setup, overall macroscopic dynamics of the system are obtained. Aggregate system variables can then be interpreted both as outcomes of and as contexts for the agents' decisions and actions (Kohler and Gumerman, 2000). As described in Bousquet and Le Page (2004), the mathematical analysis of an ABM, however, is not straightforward, unless the model is extremely simplified and general. In fact, validation of an ABM is classically done by simply running simulations (enabled by the rise of computational power in the recent decades), obtaining aggregated system variables and comparing them with observations or testing them for plausibility.

**Advantages with respect to ODE Models.** ABMs are applied to study complex systems, i.e. systems consisting of multiple components interacting with each other and, thereby, creating feedback loops and non-linearities, because of which the behaviour of the system can not be easily inferred from the input of the model. In such systems, ABMs are typically advantageous over macroscopic system models by accounting for the following system properties (Bookstaber, 2019):

- Emergent phenomena from local, heterogeneous behaviour of the agents,
- Computational irreducibility of agent behaviour (e.g. in the decision making in times of crisis),
- Non-ergodicity of relations between agents and their environment, i.e. conditions and rules of behaviour co-evolve with the agent and environment (Kohler and Gumerman, 2000),
- Stochasticity in actions and decision making processes, due to imperfect knowledge or uncertainty of the agents.

Additionally, ABMs allow for a very natural and flexible implementation<sup>1</sup> of an explicit space dependency of rules and a spatially heterogeneous environment. In particular, if a system exhibits emergent phenomena, crucial information is lost when the heterogeneity of agents is reduced to one representative agent by averaging, as done in macroscopic ODE models (Bonabeau, 2002). Instead, an ABM generates emergence from bottom-up by accounting for non-linear feedbacks due to heterogeneous agents and stochasticity.

**Application in Socio-Ecological Systems.** ABMs have traditionally been applied to problems connected to flows, markets, organisations, or diffusion (Bonabeau, 2002). Typical applications include e.g. traffic jams, ant colonies or swarm behaviour of fish and bird flocks. However, ABMs are also a common approach for socio-ecological systems (Müller-Hansen et al., 2017). Such a system comprises complex co-evolution of the heterogeneous humans and environment, which interact with each other in non-linear, adaptive ways on multiple time and spatial scales, making it suitable for the application of ABMs (Bousquet and Le Page, 2004).

**Application for Ancient Civilisations.** Agent-Based Modelling has also been applied to study the history of two ancient civilisations. Axtell et al. (2002) and Janssen (2009), used an ABM to reproduce the spatio-temporal history of the Anasazi society in a valley in Arizona, US, and its disappearance around 1300 A.D.. Agents in the model represent households with various heterogeneous attributes that interact with the environment via farming. The environment is determined from an extensive data record of harvest yield potential in the valley over time and the Agent-Environment interaction is based on this

---

<sup>1</sup>Compare for example with the unintuitive diffusion process in the ODE model by Basener et al. (2011).

yield and a set of anthropologically plausible rules. Agents choose a location for a farm depending on the maximum potential yield in a certain distance to water and for the nearest possible settlement with access to water. The harvest success determines the fertility and, thus, the dynamics of agent numbers and overall population in the valley. Heckbert (2013) developed an ABM for the Maya civilisation resulting in a ‘somewhat analogous’ reproduction of the spatial pattern and timeline. The agents in this model generate a certain amount of agricultural yield on a discretised map based on a benefit-cost assessment. They are further connected in clustered, adaptive trade networks, from which they benefit. Both of these approaches by Axtell et al. (2002) and Heckbert (2013) attempted to explain the spatio-temporal history of an ancient civilisation by developing an Agent-Based Model with anthropological rules and a biologically, geographically explicit environment on a discretised map.

**Motivation for Applying an ABM on Easter Island.** This thesis presents a similar Agent-Based modelling approach for the history of Easter Island. I have discussed many aspects and advantages of ABM, which apply in socio-ecological systems, and for modelling ancient societies (and Easter Island in particular). Similar to the valley of the Anasazi, Easter Island is a small, confined space with distinct geographical and biological features with heterogeneous agricultural suitability. Merico (2017) further argues for the use of an ABM for Easter Island to overcome the shortcomings of ODE models and limits of the available archaeological and palynological data. The main features of the ABM presented here, thus, include a spatially explicit environment, locally confined agent-environment interaction, a simple adaptation strategy of agents to environmental degradation and individual, stochastic moving decisions by agents.

# Chapter 3

## Development of an Agent-Based Model for Easter Island of Human Resource Interaction

### 3.1 Model Overview

**General Description.** I present an Agent-Based Model (ABM) that simulates the spatial and temporal history of household agents on Easter Island and their interactions with the natural environment. The environment is encoded on a 2D discretised map with heterogeneous geographic and biological features. Agents rely both on a limited, non-(or slowly) renewable resource, the palm trees, and a limited resource, farming conducted on arable land (in particular, sweet potatoes). Agents obtain these resources by cutting trees and farming viable sites in their near surroundings and, thereby, changing their local environment. Consequently, the household's population growth or decline depends on the success of this resource acquisition. Furthermore, resource availability and other geographic indicators determine the moving behaviour of the agents. The interaction with the natural environment, thus, constrains the moving patterns as well as the dynamics of the population size of the Easter Island society.

**Handling of Events and Time.** The model assumes yearly updates of the characteristic variables of each household agent and the environment throughout the simulated time period. The simulation starts with the arrival of the first settlers at Anakena Beach in

$$t_{\text{arrival}} = 800 \text{ A.D. ,} \quad (3.1)$$

following Bahn and Flenley (2017)<sup>1</sup>. The initial population is assumed to be  $\text{pop}_{\text{arrival}} = 40$  individuals (as in Brander and Taylor, 1998, and similar to Brandt and Merico, 2015) spread on 2 households, that both settle close to Anakena Beach (in the North, see Figure 1.1). After each time step,  $\Delta t = 1 \text{ yr}$ , all agents are updated and interact with their local environment sequentially in a randomised order. New household agents can appear throughout the simulation following reproduction and splitting of existing agents. Following the alteration of the environment by all agents, the environment's state variables are updated (e.g. potential regeneration, or soil degradation) once per year ('environmental update'). The simulation ends in 1900 A.D. with the arrival of frequent European voyagers, slave trade and European diseases marking the end of the isolated status of the historic Easter Island society .

**Chapter Overview.** In Section 3.2, I describe the generation of the 2D discretised map comprising the environment of Easter Island as well as the yearly environmental updates. I then focus on the household agents and the update procedure of a single agent: This comprises the calculation of agent specific features (Section 3.3), the interaction between an agent and the environment (Section 3.4), and the consequent response of the agent's features to the harvest, i.e. population growth or decline (Section A) and potential relocation (Section 3.6). Figure 3.1 summarises all environmental variables, the agent variables, and their dependencies (except for relocation, described in Figure 3.10).

---

<sup>1</sup>Other arrival dates are discussed in Section 3.5.

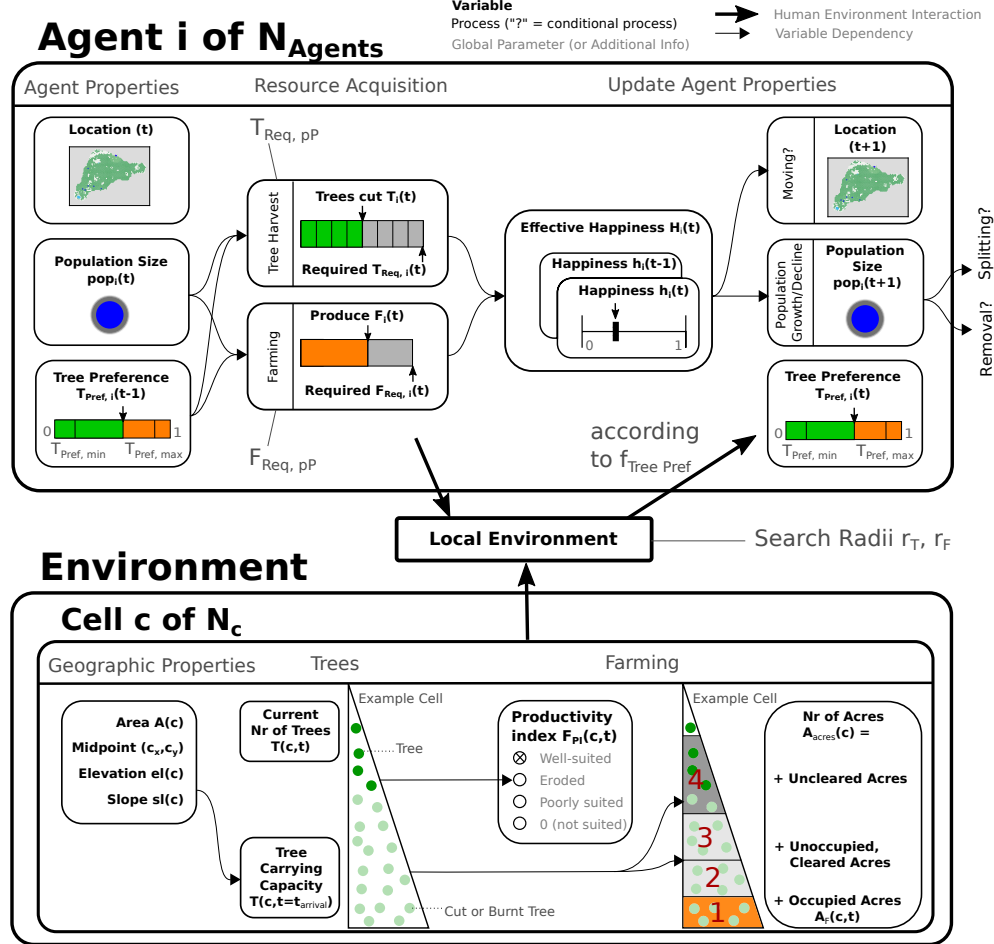


Figure 3.1: Sketch of an update of agent  $i$ . The environment consists of  $N_c$  discretised cells (triangles),  $c$ , with certain geographic properties: Area  $A(c)$ , midpoint  $\vec{c}$ , terrain elevation  $el(c)$ , and slope  $sl(c)$ . A cell has two ‘resource stocks’: The first is the number of trees  $T(c, t)$ , with a maximum of the cell’s carrying capacity (and initial state)  $T(c, t = t_{arrival})$ , which depends on  $el(c)$  and  $sl(c)$ . The second is the number of arable sites,  $A_{acres}(c)$  with a basic unit area of 1 acre, consisting of (1) uncleared, (2) cleared but unoccupied, and (3) occupied sites ( $A_F(c, t)$  in acres) and the corresponding Farming Productivity Index,  $F_{PI}(c, t)$ , of the cell. Agent  $i$  represents a household with a settlement location  $(x_i, y_i)(t)$  (corresponding cell  $c_i(t)$ ), a population size  $pop_i(t)$ , and a tree preference  $T_{Pref, i}(t - 1)$ , reflecting the state of the local environment in the previous year. The latter two (together with global, tunable per person resource requirement constants,  $T_{Req, pP}$  and  $F_{Req, pP}$ ) determine the agent’s requirements for tree cutting,  $T_{Req, i}(t)$  and farming,  $F_{Req, i}(t)$ , each year. If the location of the agent allows open-ocean fishing, the farming requirement,  $F_{Req, i}(t)$  is immediately fulfilled without occupying arable sites. The success of the resource acquisition,  $T_i(t)$  and  $F_i(t)$ , given the local environment (characterised by resource search radii  $r_T$  and  $r_F$ ) then determines the current and effective happiness of the agent,  $h_i(t)$  and  $H_i(t)$ . The latter then determines the agent’s population dynamics (including potential splitting or removal of the agent) and potential relocation of the settlement (according to a semi-rational decision making process sketched in Figure 3.10). Finally, the tree preference,  $T_{Pref, i}(t)$  is updated according to a function  $f_{Tree\_Pref}$  of the change of the local environment.

## 3.2 A Discretised Map of Easter Island with Geographical and Biological Features

**Map Discretisation.** I create a discretised map dividing the island into a number of small 2D triangular cells with certain geographical features. First, I define an equidistant grid on Easter Island<sup>2</sup> with a grid size of  $\delta_x \approx 320$  m between points in  $x$ - (i.e. 75 points) and  $\delta_y \approx 360$  m in  $y$ -direction (i.e. 50 points). In principle, the map can be created with any arbitrary resolution, constrained only by the resolution of the underlying geographical data. Also other grid types, e.g. with adaptive  $\delta_{x,y}$  to focus on regions of interest, are compatible with the model. While a higher resolution increases detailed geographical representation and reduces discretisation errors, computation time of the presented model scales highly non-linearly (see Section 3.6). Hence, a trade-off has to be found between detail or accuracy and computation time. Next, I create 2D triangular cells from this grid using *matplotlib*<sup>3</sup>'s Delaunay triangulation package. A cell  $c$  is characterised by its midpoint  $\vec{c} = (c_x, c_y)$ . Since all cells are Delaunay triangles, their smallest angles are maximised and the midpoint,  $\vec{c}$ , provides a reasonable representation of the cell. Features of the terrain, elevation,  $el(c)$ , and slope,  $sl(c)$ , of Easter Island are obtained from a publicly available, high resolution elevation map (Jarvis et al., 2008) via the Google Earth Engine interface<sup>4</sup> and evaluated at the corresponding midpoint  $\vec{c}$ . All cells located on the ocean (i.e.  $c$  with  $el(c) = 0$ ) are masked out and discarded. The cells corresponding to the island's three small crater lakes are also identified. The remaining cells constitute the landmass of the discretised island, which can be settled, deforested or farmed by the agents. With the resolution given above, a total of  $N_c = 2768$  cells are considered with an area of roughly  $A(c) = 0.06 \text{ km}^2 = 14.2 \text{ acre}$  each. The total area of the obtained discretised Easter Island map is  $A = 159.2 \text{ km}^2$ , ( $163.6 \text{ km}^2$  in reality) providing a detailed, cellular representation of geographical features (location  $\vec{c}$ , area  $A(c)$ , elevation  $el(c)$ , and slope  $sl(c)$ ).

**Trees.** Each cell  $c$  on the discretised map contains a number of trees, denoted as  $T(c, t)$  (or tree density  $T(c, t)/A(c)$ ). The island's forest system is assumed to be in equilibrium at the time of the arrival of the first settlers,  $t_{\text{arrival}}$ , and, thus,  $T(c, t = t_{\text{arrival}})$  is the constant carrying capacity of palm trees for each

---

<sup>2</sup>Ranging 18 km in latitudinal (from  $-27.2050^\circ N$  to  $-27.0437^\circ N$ ) and 24 km in longitudinal direction (from  $-109.4650^\circ E$  to  $-109.2227^\circ E$ )

<sup>3</sup>Hunter (2007)

<sup>4</sup>Gorelick et al. (2017)

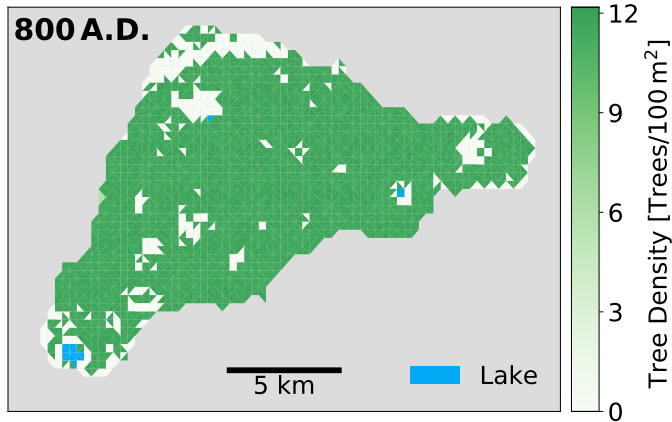


Figure 3.2: The tree density in each cell at carrying capacity (prior to the arrival of the first settlers),  $T(c, t_{\text{arrival}})/A(c)$ .

cell  $c$  on the island (c.f. Brander and Taylor, 1998). There is still some uncertainty about the total number and spatial patterns of palm trees at  $t = t_{\text{arrival}}$ . Mieth and Bork (2015) estimated a total of  $16 \cdot 10^6$  trees covering 80% of the island from observed root casts in the soil, whereas e.g. Brandt and Merico (2015) initialise the model with a conservative estimate of  $8 \cdot 10^6$  trees. Most studies assume an island wide, dense distribution of the palm trees. E.g. Bahn and Flenley (2017) stated that soil sufficient for tree growth is present ‘almost everywhere on the island, apart from the steepest parts of the cliffs and the youngest lava surfaces’ (i.e. the highest elevations of Mount Terevaka). However, Rull (2020) also investigated the possibility of variable, mosaic vegetation patterns with high densities of trees around the lakes and the coastal areas. The model presented here can incorporate any pattern of pre-arrival tree density. For this thesis, I assume a total<sup>5</sup> of

$$T(t = t_{\text{arrival}}) = \sum_c T(c, t = t_{\text{arrival}}) = 16 \cdot 10^6 \quad (3.2)$$

trees distributed according to an equal density pattern excluding those cells with very high elevation or slope ( $el(c) > 450 \text{ m}$  or  $sl(c) > 10^\circ \Rightarrow T(c, t) = 0$ ). A resulting map of pre-arrival tree numbers  $T(c, t_{\text{arrival}})$  in cells  $c$  extending on 86% of Easter Island is shown in Figure 3.2.

**Tree Dynamics.** Through anthropogenic deforestation, the variable tree number in each cell,  $T(c, t)$ , declines. Natural removal (e.g. through a changing

---

<sup>5</sup>Bold symbols denote iterations over all cells (or agents) in the thesis.

climate) is not considered in the model. In the literature on Easter Island, there seems to be a consensus between the two major contrasting theories that rats effectively hindered tree regrowth by feeding on palm nuts (e.g. Bahn and Flenley, 2017; Hunt, 2007). In line with this argument, forest regeneration does not occur in the standard configuration of this model. Trees, therefore, constitute an entirely non-renewable resource in this setting. However, I also conduct alternative experiments, in which the forest can hypothetically regenerate following anthropogenic deforestation. In this alternative setting, each year, tree numbers  $T(c, t)$  in all cells  $c$  regrow logically to their (local) carrying capacity  $T(c, t = t_{\text{Arrival}})$  if there is no farming activity on the specific cells. The maximum growth rate of the palm trees is believed to be rather slow and has even been made responsible for the ecological collapse of the island by Brander and Taylor (1998). Here (in the alternative scenario), I use

$$g_T = 0.05 \frac{1}{\text{yr}}, \quad (3.3)$$

based on the estimated maximum tree regrowth rate in Brandt and Merico (2015), i.e. between  $0.02$  and  $0.07 \frac{1}{\text{yr}}$  in the absence of rats. Some cells are deforested entirely in a single update step, which disables logistic regeneration. However, with seeds being transported to the empty cell e.g. through wind, birds or human activity, forests regrow even in empty land. To incorporate this, a small number of trees ‘pops up’ ( $0.5\%$  of the cell’s carrying capacity) after a treeless cell has been left barren, i.e. without any farming activity, for 10 consecutive years. In summary, in this model the tree number in a cell  $c$  either (standard configuration) does not regenerate at all or (alternative configuration) regenerates as

$$T(c, t+1) = \begin{cases} T(c, t) + T(c, t) \cdot g_T \cdot \left(1 - \frac{T(c, t)}{T(c, t_{\text{Arrival}})}\right) & \forall c \text{ with } \mathbf{A}_F(c, t) = 0 \\ 0.005 \cdot T(c, t_{\text{Arrival}}) & \forall c \text{ with } T(c, t) = 0 \text{ and} \\ & \mathbf{A}_F(c, \hat{t}) = 0 \ \forall \hat{t} \in \{t-10, \dots, t\} \\ 0 & \text{else} \end{cases} \quad (3.4)$$

(neglecting anthropogenic deforestation). These two scenarios, labelled as ‘without’ and ‘with’ forest regeneration, allow for testing of the impact of the Polynesian rats, assuming that they effectively hindered tree regeneration.

**Farming Sites.** Next to the resource trees, the environment also provides land for active farming of sweet potatoes<sup>6</sup> as a renewable, second resource (similar to the model of D'Alessandro, 2007). A single farming site on arable land has a constant, basic unit area of 1 acre on a cell. Hence, if a cell is arable, it provides the possibility for

$$A_{\text{acres}}(c) = \text{Rounded Down} (A(c)[\text{acres}]) \quad (3.5)$$

farming sites, which can each be occupied and farmed by an agent. The number of occupied sites in each cell is denoted as  $A_F(c, t)$ . Each farming site provides a constant output of crop yield each year.

**Farming Productivity Index.** The farming productivity per area, i.e. the potential crop yield, is strongly location dependent. Here, I define a (relative) Farming Productivity Index,  $F_{\text{PI}}(c)$ , for each cell  $c$  (shown in Figure 3.3). While the total potential of farming productivity remains uncertain (as described in the Introduction), some studies used agricultural modelling based on elevation, climate and soil quality data to obtain a more detailed, spatially explicit classification of the farming suitability:

- Puleston et al. (2017) created a map (Figure 4 in the publication) indicating regions that meet a certain viability criterion for sweet potato cultivation. This criterion marks 19% of the island as agriculturally viable, mainly in the lowland, coastal region. In this model, I denote all cells of the discretised map, which are located in this region ‘well-suited’ and assign a high farming productivity index  $F_{\text{PI}}|_{\text{well}}$ . Additionally, the map reported by Puleston et al. (2017) includes areas that did not meet the criterion but in which small, patchy areas of agricultural structures were identified from satellite images. Consequently, the yield from these regions must have been low such that the farmers used techniques like labour intensive, large-scale lithic mulching, which mainly increased moisture availability, and efficient crop management, e.g. plant spacing and frequent fallowing (Louwagie, Stevenson, and Langohr, 2006). I call all cells in this region ‘poorly suited’ and assign a low farming productivity index  $F_{\text{PI}}|_{\text{poor}}$ .
- Louwagie, Stevenson, and Langohr (2006) developed a classification for successful cultivation of several crops based on climate and soil

---

<sup>6</sup>Sweet Potato was the dominant staple crop on Easter Island (at least in later phases) (Louwagie, Stevenson, and Langohr, 2006)

property measurements at a few sites on the island and assigned relative yields to these sites. The majority of the measurement sites located at the foots of smaller craters along the arable coasts correspond partly with the well-suited and partly the poorly suited regions<sup>7</sup>. For most climatic conditions these were classified as mostly ‘marginally to moderately suitable’ for sweet potato cultivation (corresponding to a relative yield of around 55% (20 – 80%) of an optimal farming site) and, especially in wet years, some locations were classified as ‘highly suitable’ (relative yield of > 80%). One of the studied sites (‘Vaitea’), located in the poorly suited region, was found ‘not suitable’ for farming due to insufficient nutrition availability (relative yield of 0 – 20%) despite archaeological evidence of gardens in this area. Based on these results, which provide the best estimate available, I choose

$$\begin{aligned} F_{\text{PI}}|_{\text{well}} &= 80\% && \text{for well-suited (highly to moderately suitable)} \\ F_{\text{PI}}|_{\text{poor}} &= 10\% && \text{for poorly suited (not suitable)} \\ F_{\text{PI}}|_{\text{non-viable}} &= 0\% && \text{for non-viable sites} \end{aligned}$$

depending on a cell’s classification by Puleston et al. (2017) into well-suited and poorly suited cells. Hence, the total resulting arable land area in this model (shown in Figure 3.3) is ca. 29 km<sup>2</sup> (i.e. 18% of the total island area) for well-suited sites and, additionally, 50 km<sup>2</sup> (i.e. 31% of the total island area) for poorly suited sites with low Farming Productivity Index.

**Erosion.** Soil erosion through radical deforestation and heavy rainfalls degraded the farming productivity of Easter Island especially in the later phase (e.g. Brander and Taylor, 1998; Mieth and Bork, 2005; Bahn and Flenley, 2017). As trees are removed from a region, rain can wash away nutrient-rich soil and reveal less fertile ground with reduced relative yield. In the model, I assume that, if a well-suited cell is entirely deforested, the land erodes and, thus, the cell’s  $F_{\text{PI}}(c)$  reduces to

$$F_{\text{PI}}|_{\text{eroded}} = 50\% \quad \text{for well-suited cells with } T(c, t) = 0 . \quad (3.6)$$

This soil degradation is reverted as soon as trees pop back up (i.e. if the cell has been kept barren (without farming) for 10 years as described in equation 3.4).

---

<sup>7</sup>Comparing roughly Figure 1 of Louwagie, Stevenson, and Langohr (2006) with Figure 4 of Puleston et al. (2017).

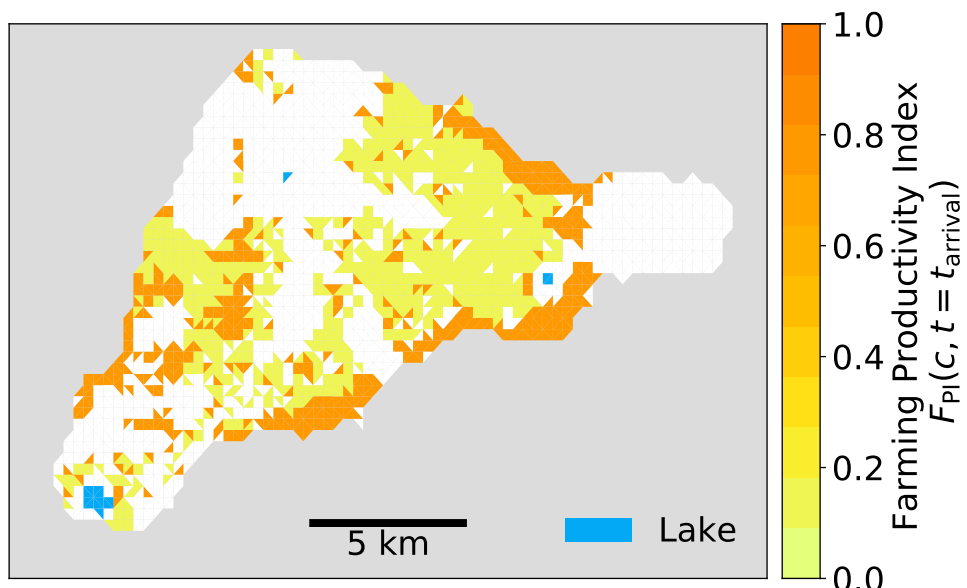


Figure 3.3: A map of the (sweet potato) Farming Productivity Indices,  $F_{PI}(c)$ , in each cell of the discretised map of Easter Island. The model makes use of the map of Puleston et al. (2017) classifying arable land into viable areas (here ‘well-suited sites’), non-viable but nevertheless partially farmed (here ‘poorly suited sites’), and non-viable sites derived from an agricultural model of climate and soil quality. This classification is combined with measurements of land suitability in several sites (Louwagie, Stevenson, and Langohr, 2006) giving rise to a simple, spatially explicit map of farming potential parametrised by the Farming Productivity Index  $F_{PI}(c)$ .

### 3.3 Human Agents and their Features

**Basic Variables.** The ABM consists of a variable number of agents,  $N_{\text{Agents}}(t)$ , which represent households, situated on the discretised map derived in Section 3.2. An agent with index  $i$  has several features describing its state at time  $t$ : The settlement is located at

$$\vec{x}_i(t) = (x_i, y_i)(t) \quad (3.7)$$

on the discretised map and, hence, associated with one specific cell  $c_i(t)$ . The agent's population size, i.e. the number of individuals in the household,

$$pop_i(t) \quad (3.8)$$

typically ranges from 12 to about 42. Macroscopic island-wide aggregate variables, like population size, are simply obtained by summation over all agents, which I denote with bold symbols (equivalent to summation over cells).

**Resource Search Radii.** Agents have access to two different types of resources, trees (and consequent derivate products) and farmed products, by interacting with their local environment defined by fixed resource search radii. Hence, the local environment of agent  $i$  is defined as:

$$C_T(c_i(t)) = \{\tilde{c} \mid \|\tilde{c} - \vec{x}_i(t)\| \leq r_T\} \quad (3.9)$$

for the resource tree with search radius  $r_T = 2$  km and

$$C_F(c_i(t)) = \{\tilde{c} \mid \|\tilde{c} - \vec{x}_i(t)\| \leq r_F\} \quad (3.10)$$

for occupying farming sites with radius  $r_F = 1$  km.

**Tree Preference.** The agent's total required resource uptake is split between tree cutting and farming yield, given by a trait parameter, the tree preference  $T_{\text{Pref}, i}(t)$  for agent  $i$  at time  $t$ , which reflects the state of the local environment. In the first phase of settling on the island, the civilisation mainly lived off the island's abundant natural resources (here trees) (Bahn and Flenley, 2017). However, over time, the economy 'switched from predominantly hunter-gatherer to a dryland farming society' (Louwagie, Stevenson, and Langohr, 2006). The tree preference trait,  $T_{\text{Pref}, i}(t)$ , in this model is designed such that agent's adjust their harvest behaviour for next year given the current state of the local environment (in particular the level of deforestation). Hence, as trees are removed

from an agent's local environment and more arable land is cleared freeing up space for agriculture, the agent's tree preferences decrease and its farming requirement increases accordingly. In this model,  $T_{\text{Pref}, i}(t)$  depends on the relative change of tree density with respect to the initial state at  $t = t_{\text{arrival}}$  in the local environment:

$$T_{\text{Pref}, i}(t) = f_{\text{Tree Pref}} \left( \frac{\sum_{\tilde{c} \in C_T(c_i(t))} T(\tilde{c}, t)}{\sum_{\tilde{c} \in C_T(c_i(t))} T(\tilde{c}, t_{\text{arrival}})} \right) \quad (3.11)$$

The shape of the function  $f_{\text{Tree Pref}}$  is an indicator of the adaptation strategy of the economy/society to environmental change. How fast do agents adapt their harvest behaviour, when the non-renewable resources, trees, are depleted? I consider four strategies (shown in Figure 3.4): The tree preference  $T_{\text{Pref}, i}(t)$  decreases

- linearly with the local, relative tree density decline (linear case).
- delayed with the local, relative tree density decline (delayed case).
- faster than the local, relative tree density decline (faster or careful case),
- first delayed, and at some point faster than the local, relative tree density decline (logistic case)

The tree preference is limited to a certain range, assuming an agent can not live purely off trees (and associated derivate products), but, at the same time, some tree cutting is always required even for maximum agricultural production (e.g. as cooking wood or for tools). Here, I choose:

$$T_{\text{Pref, min}} = 0.2 \quad \text{and} \quad T_{\text{Pref, max}} = 0.8 \quad (3.12)$$

In the standard configuration in this model, I use the linear relation and, hence,

$$T_{\text{Pref}, i}(t) = \frac{\sum_{\tilde{c} \in C_T(c_i(t))} T(\tilde{c}, t)}{\sum_{\tilde{c} \in C_T(c_i(t))} T(\tilde{c}, t_{\text{arrival}})} \cdot (T_{\text{Pref, max}} - T_{\text{Pref, min}}) + T_{\text{Pref, min}} \quad (3.13)$$

Initially, agents start with maximal tree preference ( $T_{\text{Pref}, i}(t = t_{\text{arrival}}) = T_{\text{Pref, max}} \forall i$ ), which then (in general) decreases slowly as deforestation progresses.

**Resource Requirements.** An agent's required total resource uptake per year increases with the population size and the tree preference calculated after the

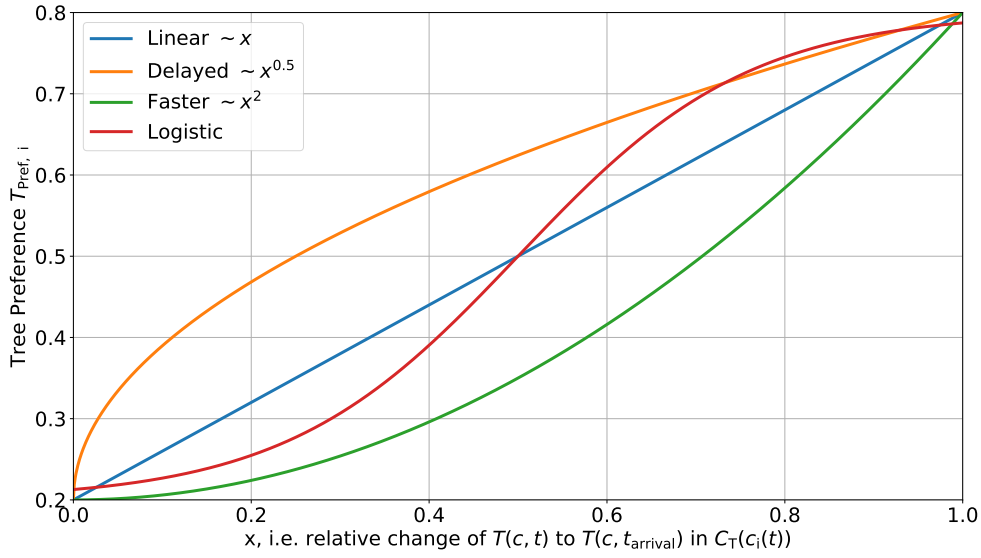


Figure 3.4: Relationships of an agent's tree preference,  $T_{\text{Pref}, i}(t)$ , with respect to relative changes in local tree density for the four considered adaptive strategies  $f_{\text{Tree Pref}}$  with  $x$  given in equation 3.11.

harvest in the previous year. Hence, the resource requirements of tree harvest,  $T_{\text{Req}, i}(t)$ , and farming produce,  $F_{\text{Req}, i}(t)$ , are

$$T_{\text{Req}, i}(t) = T_{\text{Pref}, i}(t - 1) \cdot \text{pop}_i(t) \cdot T_{\text{Req}, \text{pP}} \quad (3.14)$$

and, similarly,

$$F_{\text{Req}, i}(t) = (1 - T_{\text{Pref}, i}(t - 1)) \cdot \text{pop}_i(t) \cdot F_{\text{Req}, \text{pP}}, \quad (3.15)$$

where  $T_{\text{Req}, \text{pP}}$  is the constant tree requirement per year per person in absence of agriculture and  $F_{\text{Req}, \text{pP}}$  is the constant required agriculture production per person in the absence of tree cutting.

The tree requirement per person (in the absence of farming),  $T_{\text{Req}, \text{pP}}$ , in principle depends on a multitude of factors and was presumably heterogeneous among agents. E.g. if agents used sugary sap from cut tree trunks as freshwater replacement (as suggested by Mieth and Bork, 2015), they would require a much larger number of trees. Here, I use a constant parameter of

$$T_{\text{Req}, \text{pP}} = 5 \frac{\text{Trees}}{\text{person} \cdot \text{yr}} \quad (3.16)$$

for all agents (for the standard configuration) based on the maximum harvest

rate used in Brandt and Merico (2015), about 3 to 7 trees per year<sup>8</sup>. However, I also explore a scenario with doubled tree requirement per person per year. The requirement of farmed land per person (in the absence of tree cutting),  $F_{\text{Req, pP}}$ , crucially determines the overall carrying capacity of the human population. Puleston et al. (2017) simulate the nutritional productivity of farming on well-suited land (as defined in Section 3.2) for two different environmental scenarios of Nitrogen fixation in the soil, i.e. the rate at which Nitrogen is renewed, which represents a major uncertainty in their model<sup>9</sup>. This can be converted into the land required by one individual using the nutrition content of sweet potato<sup>10</sup>:

$$F_{\text{Req, i}}(t) = \begin{cases} 0.5 \frac{\text{acre}}{\text{person}} & \text{for high N fixation} \\ 1.7 \frac{\text{acre}}{\text{person}} & \text{for low N fixation} \end{cases} \quad (3.17)$$

However, the actual amount of required land per individual in the model is higher since all acre have less than 100% relative yield (see definition of farming productivity indices  $F_{\text{PI}}(c)$  and Figure 3.3).

In summary, the resource requirements for trees (in absolute numbers) and farming produce (in acres of farmed sites with 100% yield) are agent-specific, yearly updated features depending on the population size, reflecting the state of last year's local environment via the tree preference, and which can be tuned through the global parameters  $T_{\text{Req, pP}}$  and  $F_{\text{Req, pP}}$ .

**Fishing.** The model, furthermore, allows for open-ocean fishing as a replacement for farming for some agents living near the coast at Anakena Beach (see Figure 1.1). Instead of farming sites, these fishers gain sufficient agricultural resources by going out to sea on large canoes. Excavations prove that shellfish, fish, and even porpoise were a major part of the Easter Islanders' diet during the first settling phase (Bahn and Flenley, 2017). As a resource management institution the Easter Island society installed taboos on the harvest of natural resources to confine overexploitation (Good and Reuveny, 2006). Fishing was mainly restricted to members of a specific chiefdom ('Miri') living at Anakena Beach (Bahn and Flenley, 2017) who would then presumably trade with others. Hence, in the model, every agent up to a maximum of  $N_{\text{Fisher, Max}} = 10$

---

<sup>8</sup>Brandt and Merico (2015) use a only half of the initial trees before arrival of the first settlers, though)

<sup>9</sup>I do not consider fallowing as farming practice to increase productivity of arable land, as this, in general, reduces the productivity per total occupied area needed for each individual (see Table 1 in Puleston et al., 2017).

<sup>10</sup>1 t/yr roughly sustains 1 individual in the absence of other food sources

(i.e. typically less than 400 individuals) living within radius,  $r_F$ , from Anakena Beach (in cell  $c_{\text{Anakena}}$ ) automatically becomes a fishing agent

$$c_i \in C_F(c_{\text{Anakena}}) \cup N_{\text{Fishers}} < N_{\text{Fisher, Max}} \Rightarrow \text{Agent } i \text{ becomes a fisher} \quad (3.18)$$

While I assume that open-ocean fish supply is unlimited for those living at Anakena Beach, the major constraint for the fishers is the requirement for trees. Since e.g. the construction of canoes or firewood presumably increased the tree requirement of these agents, I increase the minimum tree preference to

$$T_{\text{Pref, min}}|_{\text{fisher}} = 0.5. \quad (3.19)$$

Hence, while fishing agents near Anakena Beach do not have any farming requirements due to access to an unlimited resource stock from the sea, the correspondingly higher requirement for trees and an externally introduced restriction on their number limit the exploitation of open-ocean fishing.

## 3.4 Agent-Environment Interaction

**Sequence of Events.** At any time  $t$ , an agent first determines the required amount of trees,  $T_{\text{Req, i}}(t)$ , and agricultural production,  $F_{\text{Req, i}}(t)$ , (as described in Section 3.3) and then acquires sufficient resources (if available) by interacting with the local environment, i.e. by occupying sites for farming and removing trees. This interaction is described in the remaining Section. The sketch in Figure 3.5 shows an example of the process of deforestation and consequent establishment of farming in a cell.

**Farming.** An agent occupies arable land unit sites,  $A_{F, i}(t)$ , with a fixed area of 1 acre associated to one cell and obtains a yearly farming produce of

$$F_i(t) = \sum_{a \in A_{F, i}(t)} F_{PI}(c(a)), \quad (3.20)$$

where  $a$  denotes a farmed acre and  $c(a)$  is the corresponding cell of this acre<sup>11</sup>. Agents keep all their currently occupied sites  $A_{F, i}(t)$  until the next year. If, over time, an agent  $i$ 's farming requirement,  $F_{\text{Req, i}}(t)$ , increases e.g. due to population growth, decrease of the tree preference or erosion of the soil of one of its occupied sites, and consequently the farming produce of the previous

---

<sup>11</sup>Note, for fishers  $F_i(t) = F_{\text{Req, i}}(t)$  holds immediately without farming and occupying sites.

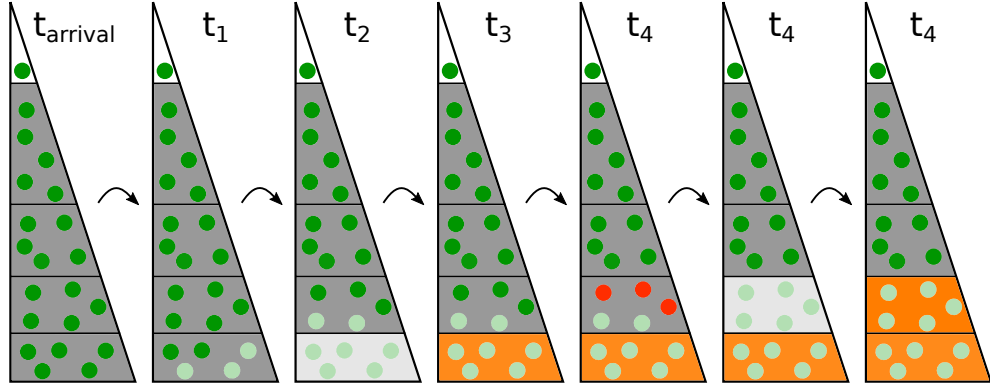


Figure 3.5: Example of deforestation (by arbitrary agents) in a cell  $c$  (black triangle) with an area of 4.2 acres. The cell is arable, with  $F_{PI}(c) > 0$  and, thus, provides  $A_{acres} = 4$  acres for potential farming (grey areas). Initially at  $t_{arrival}$ , the cell has 21 trees (carrying capacity). At some time  $t_1$ , after deforestation 18 of these trees still exist. An Agent  $a$  cuts 4 more trees in the cell ( $\rightarrow t_2$ ). Subsequently, Agent  $b$  occupies the cleared site (1 acre, light grey area) for farming (orange area) ( $\rightarrow t_3$ ). Finally, an agent  $c$ , needs to clear 3 trees by burning them (red dots) to occupy a second acre on this cell to fill its farming requirement ( $\rightarrow t_4$ ).

year would be insufficient, then the agent needs to occupy more arable sites, i.e.:

$$F_i(t-1) < F_{Req, i}(t) \Rightarrow \text{Extend } A_{F, i}(t) \text{ and, thus, } F_i(t). \quad (3.21)$$

In the search for new farming sites, an agent first considers only sites in well-suited cells, i.e.  $c \in C_F(c_i(t))$  with  $F_{PI}(c) = F_{PI}|_{\text{well}}$ , in order to maximise farming efficiency. An acre in an arable cell can only be occupied (or added to  $A_{F, i}(t)$ ) if at least this area of 1 acre is cleared off trees and not already occupied. Assuming that the trees are evenly distributed on the cell's area, the condition can be calculated as

$$\left(1 - \frac{T(c, t)}{T(c, t_{arrival})}\right) \cdot A(c) - A_F(c, t) \geq 1 \quad (3.22)$$

where the first term is the treeless area in acres and the second term,  $A_F(c, t)$ , is the number of already farmed acres (by any agent) in cell  $c$ .

If there are no well-suited sites left that fulfil this condition, the agent uses the slash and burn method to remove trees in a well-suited cell  $c$  (with at least one unoccupied acre). The agent starts burning trees on the cell that requires the least amount of trees removed for the condition to hold (without leading to soil erosion of the cell, i.e.  $T(c, t) = 0$ ). Burning trees and occupying sites continues until the farming requirement of the agent is satisfied or no more well-suited acres are available (even if this leads to soil erosion of the cell). The

use of fires to clear space is supported by the extensive charcoal record starting with the period of intensified agriculture (Mieth and Bork, 2015). Here, I assume that if space is required for farming at time  $t$ , trees are directly burned without being used for any other requirement (assuming this is a more gradual process over the year than the instantaneous burning). If, all well-suited sites within  $C_F(c_i(t))$  are occupied, but the agent's farming production does not yet meet the requirement ( $F_i(t) < F_{\text{Req}, i}(t)$ ), the agent also occupies sites on eroded cells and then on poorly suited cells in the same procedure.

**Tree Harvest.** After fulfilling the farming requirement, the agent cuts down trees according to its tree requirement  $T_{\text{Req}, i}(t)$ . An agent  $i$  selects random cells  $c \in C_T(c_i(t))$  with uniform probability and successively removes trees from these cells until the number of cut trees,  $T_i(t)$  matches the requirement  $T_{\text{Req}, i}(t)$  or no further trees are present in  $C_T(c_i(t))$ . Unlike farming, where occupied sites are kept and re-used (with the same productivity index) in the next year, the agent obviously needs to find new trees every year. While the agent's adapt their harvest behaviour via the tree preference as this non-renewable resource is depleted over time, a minimum amount of trees is always required and, hence, there's no equilibrium existence of human population without tree regrowth.

**Happiness Index.** A characteristic of the agent is happiness,  $h_i(t)$ , which reflects the success of the harvest of trees and farming production each year. Here, an agent  $i$ 's happiness  $h_i(t)$  depends on the ratios of the cut trees,  $T_i(t)$ , and farming production,  $F_i(t)$ , w.r.t. the annual requirements determined beforehand,  $T_{\text{Req}, i}(t)$  and  $F_{\text{Req}, i}(t)$ , respectively. By assuming that both resources are equally indispensable for the agent, happiness is equal to the smaller of the two fractions:

$$h_i(t) = \min \left( \frac{T_i(t)}{T_{\text{Req}, i}(t)}, \frac{F_i(t)}{F_{\text{Req}, i}(t)} \right) \quad (3.23)$$

This is also known as Liebig's law of the minimum, which states that growth is determined by the most scarce resource<sup>12</sup>. If both requirements are filled for agent  $i$ , the happiness is maximal,  $h_i(t) = 1$ . However, if either  $T_i(t) = 0$  or  $F_i(t) = 0$ ,  $h_i(t) = 0$  follows regardless of the success in harvesting the other resource. I assume that households have some resilience to a decline in harvest success (e.g. by storing food in more successful years), and, hence, define an

---

<sup>12</sup>Or: 'A chain is only as strong as the weakest link'.

effective happiness  $H_i(t)$  as

$$H_i(t) = \begin{cases} h_i(t) & \text{if } h_i(t) \geq h_i(t-1) \\ \frac{h_i(t)+h_i(t-1)}{2} & \text{if } h_i(t) < h_i(t-1) \end{cases} \quad (3.24)$$

If an agent's current harvest success decreases (due to resource scarcity), its effective happiness,  $H_i(t)$ , decreases monotonically. If e.g. all trees were to suddenly vanish within a year, an agent would have two years before its effective happiness reaches its minimum  $H_i(t) = 0$ . However, if harvest success increases (e.g. due to moving the settlement to a better location), the effective happiness takes on the current happiness value immediately. As an indicator for successful resource acquisition, the effective happiness  $H_i(t)$  determines the possible responses of agent  $i$  to the harvest, which I describe in Sections 3.5 and 3.6.

### 3.5 Population Growth

**Stochastic, Discrete Population Growth.** Following the interaction between the agent and the environment through farming and tree cutting, the agent's population size  $pop_i(t)$  adapts. The net (positive or negative) growth rate of the agent's population at a specific time depends only on the effective happiness and, thus, harvest success:

$$pop_i(t+1) = (1 + g(H_i(t))) \cdot pop_i(t) \quad (3.25)$$

In fact, instead of assuming continuous growth or decline according to this growth rate,  $g(H_i(t))$ , the population dynamics is implemented as a discrete, stochastic process. Each individual of the household agent has a  $|g(H_i(t))|$  probability to die if  $g(H_i(t)) < 0$ , or to reproduce (i.e. adding one individual to the household/agent) if  $g(H_i(t)) > 0$ . The population size stays constant at  $H_i(t) = H_{\text{equ}}$  with  $g(H_{\text{equ}}(t)) = 0$ . This results in a stepwise growth/decline of the population in which each agent's population size trajectory is a single realisation of the stochastic process which on average matches the continuous dynamics in equation 3.25 (compare e.g. with Bungartz et al., 2009). Note,  $g(H_i(t))$  represents a harvest dependent stochastic, discrete *excess* growth or decline rate. I assume that 'base' (i.e. for  $H_i(t) = H_{\text{equ}}$  and, thus,  $g(H_{\text{equ}}) = 0$ ) deaths and births average out for each year in spite of the fact that this too is a stochastic discrete process (Bungartz et al., 2009). Figure A.1 in Appendix 3.5 shows a few different realisations of a discrete, constant (excess) growth scenario with rate  $g(H_i(t) = 1) = 0.7\%$  (i.e. with unlimited resource availability) in comparison to continuous growth.

**Growth with Unlimited Resources.** There is a strong debate about the initial growth rate of the Easter Island population after the arrival of a small number of Polynesians. This corresponds to the growth rate,  $g(H_i(t))$ , without resource constraints and, thus,  $H_i(t) = 1$ . Parameters found in the literature range from 0.7% per year (Bahn and Flenley, 2017) or ‘always below 1%’ (Brander and Taylor, 1998) to more than 3% (Hunt, 2007) for short periods of time or 2.3 – 4.5% (Brandt and Merico, 2015). Depending on the proposed chronology, researchers have to make very contrary assumptions on population growth in order to fit the population dynamics to the few undisputed facts about the historic Easter Island civilisation. If an arrival around 1200 A.D. is assumed (as in Hunt, 2007, or Brandt and Merico, 2015), a large population growth is unavoidable<sup>13</sup>. Slower initial population growth needs to be assumed in studies proposing earlier arrival dates (around 800 A.D. e.g. in Bahn and Flenley, 2017), or even as early as 400 A.D. in Good and Reuveny, 2006, and Brander and Taylor, 1998)<sup>14</sup>. Other hypothesis, such as multiple, distinct periods of population growth and declines have been put forward (e.g. Cole and Flenley, 2008), but do not seem to be common in the context of Easter Island. Following Bahn and Flenley (2017), I choose an early arrival date here ( $t_{\text{arrival}} = 800 \text{ A.D.}$ ), as described before, and, thus, a slow growth rate (in one year) in the case of unlimited resource access and, therefore, continuously happy agents:

$$g(H_i(t) = 1) = 0.7\% . \quad (3.26)$$

**Growth or Decrease with Limited Resources.** The dependency of the population growth or decline rate,  $g(H_i(t))$ , in the case of limited resources, i.e.  $H_i(t) < 1$ , is a further uncertainty in modelling human-resource interactions in general. Lee and Tuljapurkar (2008) and Puleston and Tuljapurkar (2008) constructed a food-limited demography model, which was later applied to Easter Island (Puleston et al., 2017). Here I use a strongly simplified assumption of this model to parametrise the impact of non-optimal harvests on the population dynamics. The authors derived age-dependent survival and fertility rates, which are both S-shaped curves w.r.t. food availability (i.e. high in the case of unlimited food availability and low in the case of scarce food availabil-

---

<sup>13</sup>E.g. as it seems impossible that only a few hundred inhabitants in the 13th to 16th century could have created several hundred Moai statues (and caused a massive alteration of the island’s environment)

<sup>14</sup>given that archaeological data indicates an intensification of human activity, which suggests a large population size, only starting after 1200 A.D. (e.g. Bahn and Flenley, 2017 and Hunt, 2007).

ity). Since I do not consider age structures, I simply assume a net growth rate with the same shape as the survival and fertility rates in Lee and Tuljapurkar (2008).

$$g(H_i(t)) \sim \text{CDF}(\Gamma_{\text{Dist}}(\text{shape}, \text{scale} = 0.1)) \quad (3.27)$$

where  $\text{CDF}(\Gamma_{\text{Dist}})$  is the cumulative density function of the Gamma distribution (characterised by shape and scale parameter) with scale fixed as in Lee and Tuljapurkar (2008). I then tune the shape parameter of this function to obtain the same equilibrium point  $g(H_i(t) = H_{\text{equ}}) = 0$  as Puleston et al. (2017), at which the population size remains constant:

$$H_{\text{equ}} = 0.6883 \quad \text{with } g(H_i(t) = H_{\text{equ}}) = 0. \quad (3.28)$$

This corresponds to  $\text{shape} = 1.95$ , which I use in the standard configuration. In order to test sensitivity of the results w.r.t. this parameter choice, I also investigate a larger shape parameter  $\text{shape}^* = 3$  with  $H_{\text{equ}}^* = 0.84$ , which leads to a less resilient population size when resource scarcity sets in. The amplitude of the resulting function (for both scenarios) is scaled to give the chosen reproduction rate under unconstrained food supply from last paragraph  $g(H_i(t) = 1) = 0.7\%$ . Figure 3.6 shows the results of this dependency (standard setting in blue and less resilient setting in red) with the happiness regime for net growth,  $H_i(t) > H_{\text{equ}}$  (with a maximum of  $g(H_i(t) = 1) = 0.7\%$ ) and the regime for net decline of the population size,  $H_i(t) < H_{\text{equ}}$ .

**Splitting or Removal of an Agent.** There are upper and lower limits to the population size of an agent, causing it to split or disperse. If the population size  $pop_i$  of an agent  $i$  falls below a certain threshold  $pop_{\min} = 6$ , the agent  $i$  is removed and the remaining individuals are adopted by other households chosen randomly within the moving radius distance,  $r_M$  ( $C_M(c_i)$  defined later). If the household's population becomes too large, a subgroup splits from it forming a new agent. According to Bahn and Flenley (2017), settlements found in archaeological excavations consisted of two to three dwellings, the basic domestic units (e.g. caves or stone houses). Assuming that roughly a dozen people can live in such a dwelling, which would include the larger family, a household includes around 30 ( $2.5 \cdot 12$ ) individuals. In this model, if the population size reaches values requiring more than three dwellings, a dozen individuals split off and start a new settlement in a different location on the island. The stochastic splitting probability given an agent's population size is

$$Pr_{\text{splitting}} = \mathcal{N}(\mu = pop_{\max, \text{mean}}, \sigma = pop_{\max, \text{std}}). \quad (3.29)$$

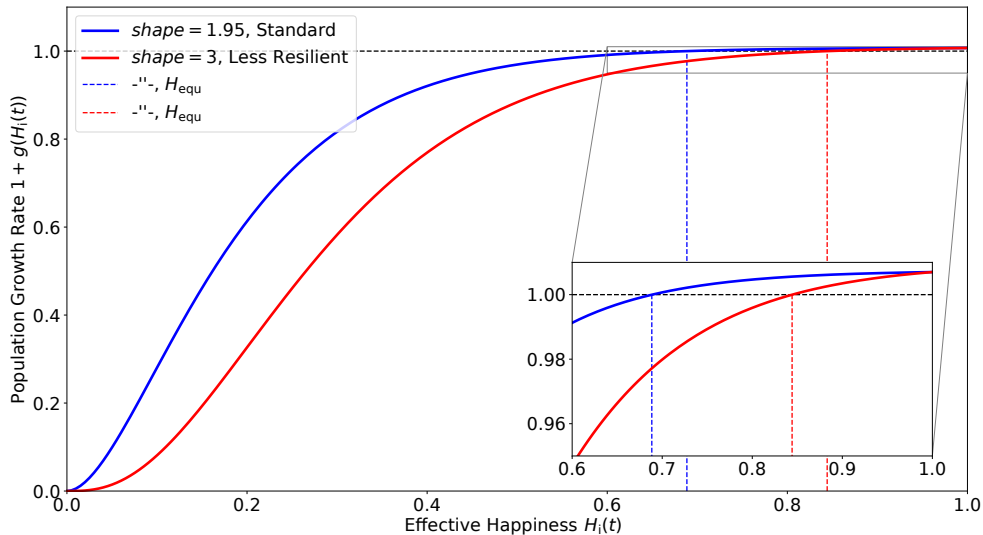


Figure 3.6: The growth rate of an agent's population size as a function of its effective happiness  $H_i(t)$ . Functional dependence follows simplified assumptions made in the food-limited demography model by Lee and Tuljapurkar (2008), Puleston and Tuljapurkar (2008), and Puleston et al. (2017). In the standard scenario (red) the agent's population size grows if  $H_i(t) > H_{\text{equ}} = 0.6883$  and declines for smaller  $H_i(t)$ . An alternative, less resilient scenario is also tested, with a smaller population growth regime of  $H_i(t) > 0.84$ . The maximum growth rate in the case of maximum happiness (and thus unconstrained resource availability) is  $g(H_i(t) = 1) = 0.7\%$ .

with Gaussian mean  $pop_{\max, \text{mean}} = 3.5 \cdot 12 = 42$  and standard deviation  $pop_{\max, \text{std}} = 3$ . The remaining household with reduced population size and, thus, smaller farming requirement then frees up no longer required sites for farming<sup>15</sup>. The splitting agent, immediately moves to a new location determined by the moving process described in Section 3.6. In summary, an agent represents a household of typically 12 (with a lower limit of 6) to 42 individuals.

## 3.6 Movement of agents

**Procedure and Condition for Moving.** Agents relocate their settlement either in response to insufficient harvest or after splitting from a large household to start a new settlement. An agent abandons the settlement if, after the harvest, its smoothed happiness is below the equilibrium point  $H_{\text{equ}} = 0.6883$  (in the standard setting), i.e. net negative population growth  $g(H_i(t)) \leq 0$ . The agent first chooses a cell within a certain radius according to probabilities that reflect how high the agent evaluates this location based on several different categories. Within this new cell, the agent chooses a location according to a uniform probability and settles there.

**Moving Radius.** In the initial phase of the simulation, agents can choose new locations from all cells on the island<sup>16</sup>. However, if a certain total population size is exceeded (here  $\text{pop}(t) \geq \text{pop}_{\text{restricted moving}} = 5000$  people), a restriction of the agents' ability to move around freely is enforced and, therefore, new settlements are only allowed within a certain radius of the agent's old location. When relocating the settlement, an agent  $i$ , thus, chooses from cells:

$$C_M(c_i, \text{pop}(t)) = \begin{cases} \{\tilde{c} \mid \tilde{c} \text{ on island}\} & \text{if } \text{pop}(t) < 5000 \\ \{\tilde{c} \mid \|\vec{c} - \vec{x}_i(t)\| \leq r_M\} & \text{else} \end{cases} \quad (3.30)$$

with radius  $r_M = 5$  km.

**Deciding on the New Location.** In a semi-rationale decision making process the agents choose a new location by evaluating cells  $c$  within  $C_M(c_i, \text{pop}(t))$  according to probabilities inferred from several different penalties:  $P_{G(c)}$  for

---

<sup>15</sup>Acres with lower farming productivity first.

<sup>16</sup>Except for the initial settlers who are assumed to settle close to the landing spot, Anakena Beach

geographical constraints,  $P_W(c)$  for distance from freshwater,  $P_D(c)$  for population density,  $P_T(c)$  for tree availability, and  $P_F(c)$  for farming land availability. High penalties represent unfavourable conditions (in the specific category) for settling in the specific cell.

**General Calculation of Penalties.** Penalties for each category  $P_X$  ( $X = \{G, W, D, T, F\}$ ) are calculated with logistic functions depending on one characteristic evaluation variable  $x$  ranging from  $x_{\min}$  to  $x_{\max}$ . In reality such an evaluation would typically depend on more than one variable and might be related to complex functional behaviour. However, the assumption made here is a plausible simplification given that with the logistic function there is a range of values of the evaluation variable indicating favourable conditions (with negligible penalties) and a range of values indicating unfavourable conditions (with high penalties)<sup>17</sup>. I determine the shape of the function of  $P_X$  of variable  $x$  through ‘thresholds’  $x_{P0.01}$  and  $x_{P0.99}$  indicating the value of  $x$  at which the penalty  $P_X$  is smaller than 1% (favourable conditions) or larger than 99% (unfavourable conditions), respectively, in this category  $X$ . The penalty  $P_X$  in a cell  $c$  with value  $x(c)$  is then

$$P_X(c) = \frac{1}{1 + \exp\left(-k_X(x(c) - \frac{x_{P0.01}+x_{P0.99}}{2})\right)} \quad (3.31)$$

where steepness  $k_X$  is

$$k_X = \left(\frac{x_{P0.99} - x_{P0.01}}{2}\right)^{-1} \cdot \log\left(\frac{0.99}{0.01}\right). \quad (3.32)$$

to fix the penalty to the respective values at thresholds  $x_{P0.01}$  and  $x_{P0.99}$ . This function is shown for a general case in Figure 3.7. For each category  $X$ , this logistic function has the same (relative) shape between  $x_{P0.01}$  and  $x_{P0.99}$ . Hence, the sensitivity of penalty  $P_X$  to differences in variable  $x$  is determined from  $x_{P0.01}$  and  $x_{P0.99}$ , and thus,  $k_X$ . If the values of  $x_{P0.01}$  and  $x_{P0.99}$  are close, equation 3.31 converges to a sigmoid function. If they are far apart, the function resembles a less steep increase of the penalty  $P_X$  with  $x$ . For  $x = \frac{x_{P0.01}+x_{P0.99}}{2}$  the penalty is  $P_X = 50\%$ . Note, that if  $x$  is chosen such that large values are favourable (e.g. for the tree and farming penalty), choosing values  $x_{P0.01} > x_{P0.99}$  simply mirrors the logistic function in equation 3.31 at

---

<sup>17</sup>For example an agent might assign the same penalty to two locations 100 m and 500 m away from a large freshwater source. If instead the nearest lake is too far away from the agent to rely on it for everyday use, alternative sources have to be found, regardless of whether the distance is 5 or 10 km and therefore, the penalty is similarly high.

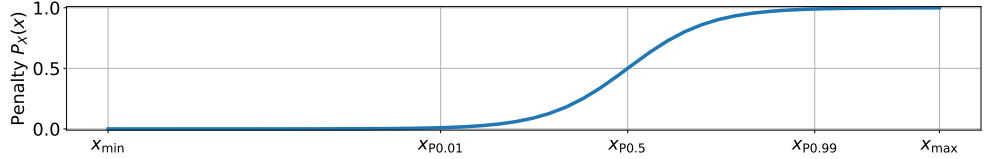


Figure 3.7: General shape of the logistic function  $P_X(c)$  for a penalty for moving to a certain cell  $c$  in the category  $X \in \{W, G, D, T, F\}$ . The penalty depends on a characteristic variable  $x$ , in combination with the thresholds,  $x_{P0.01}$  and  $x_{P0.99}$  (and  $x_{\min}$  and  $x_{\max}$ ) and, thus, the steepness parameter  $k_x$ .

its midpoint  $x = \frac{x_{P0.01} + x_{P0.99}}{2}$ . In summary, this logistic dependence of penalties on characteristic variables represents a non-linear evaluation of locations.

**Parameter Choices.** I determine the choice of the evaluation variable  $x$  and thresholds  $x_{P0.01}$  and  $x_{P0.99}$  via plausible, heuristic arguments or estimates. The following paragraphs point out the motivation for the specific variables for the agent's evaluation process and the threshold choices in the standard configuration of the model for each penalty category  $P_X$  ( $X = \{G, W, D, T, F\}$ ). Table 3.1 summarises the variables and corresponding thresholds that together with equation 3.31 determine the penalties  $P_X$  w.r.t.  $x$  for all categories and thus the decision making of an agent when relocating the settlement.

**Distance from Freshwater.** There are very limited permanent sources of freshwater on the island, making it an important factor of settlement behaviour. Nearly all studies on Easter Island history point out that the lakes inside the three volcano craters (Rano Kau in the South, Rano Raraku in the East, and Rano Aroi in the North, cf. Figure 1.1) are the main freshwater reservoirs<sup>18</sup> and, thus, are 'obvious centres for human activity' (Bahn and Flenley, 2017). Consequently, I assume that potential locations close to (large) lakes are more likely settled. The evaluation variable  $w$  radially increases with the distance to the nearest lake weighted by the lake area:

$$w = \min_{\text{lake} \in [\text{Kau, Raraku, Aroi}]} \left( \frac{\|\vec{c} - \vec{\text{lake}}(t)\|^2}{r_{\text{lake}}^2 \pi} \right) \quad (3.33)$$

---

<sup>18</sup>Other potential sources include pools in lava tubes and springs in the North Coast (all mentioned in Bahn and Flenley, 2017), an intermittent stream from Mount Terevaka, wells and water bubbles at low tide, and sugar cane juice (all mentioned in Diamond, 2011). Additionally, Mieth and Bork (2015) emphasizes the possibility to obtain a sugary sap from cut palm tree trunks, which could have replaced the need for freshwater for a large share of the population. However, crater lakes are the most reliable (and accessible) large freshwater supply.

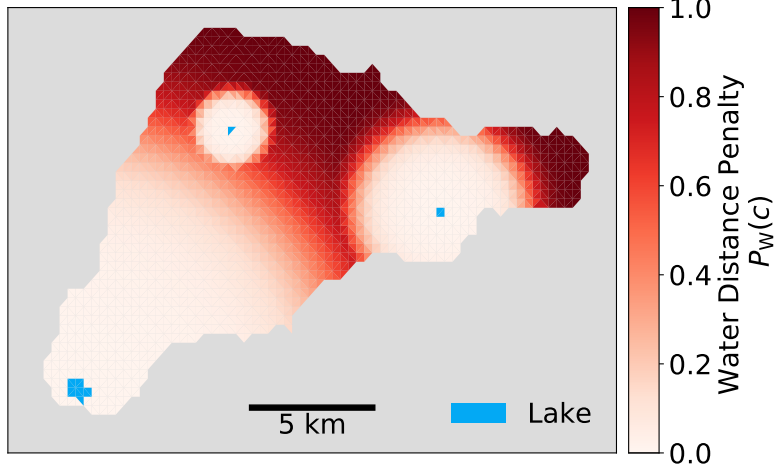


Figure 3.8: The water penalty  $P_W(c)$  for all cells in times without drought, i.e. when Rano Raraku (in the East) provides freshwater.

with  $r_{Kau} = 506 \text{ m}$ ,  $r_{Raraku} = 170 \text{ m}$ ,  $r_{Aroi} = 75 \text{ m}$  and  $\vec{lake}$  the position of the cells corresponding to the lakes. The thresholds are chosen as

$$w_{P0.01} = \frac{(0.5 \text{ km})^2}{r_{Raraku}^2 \pi} \quad w_{P0.99} = \frac{(5 \text{ km})^2}{r_{Raraku}^2 \pi} \quad (3.34)$$

(0.5 and 5 km distance of a lake like Rano Raraku, respectively). Then,  $P_W(c)$  is calculated from equation 3.31 with evaluation variable  $w$ , the corresponding thresholds and  $k_W$  as in equation 3.32:

$$P_W(c) = \frac{1}{1 + \exp\left(-k_W(w(c) - \frac{w_{P0.01} + w_{P0.99}}{2})\right)} . \quad (3.35)$$

Drought periods during the Medieval Climate Anomaly (period before 1200 A.D.) and the Little Ice Age (1570 – 1720 A.D.) potentially led to a dessication of Rano Raraku (Rull, 2020), which is also incorporated here. A map of the constant  $P_W(c)$  (without drought) is shown in Figure 3.8.

**Geographical Constraints.** High elevation and slope of Easter Island further penalise the settlement probabilities in this model. Archaeological evidence (e.g. the distribution of the Ahu and Moai) shows that the first 1 – 2 km inland from the coast were the preferred settlement locations, even if upland locations were farmed (Bahn and Flenley, 2017). There are several possible

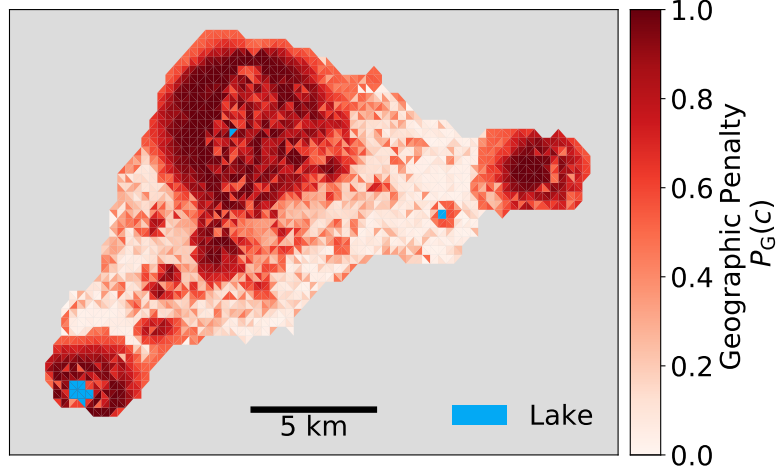


Figure 3.9: The constant geography penalty  $P_G$  for all cells.

reasons for that including easier access to small-scale fishing, climatic conditions, or cultural reasons. Hence, I assume that the geographical penalty depends on a cell's elevation. The evaluation variable is  $el(c)$  and the chosen thresholds  $el_{P0.01} = \min_c(el(c)) = 0\text{ m}$  and  $el_{P0.99} = \max_c(el(c)) = 300\text{ m}$  (arbitrary choice). Furthermore, the North West coast and the areas around the volcano craters are steep, making it difficult for large households to settle in these spots, e.g. due to the danger of land slides. Hence, the geographical penalty also depends on a cell's slope. The evaluation variable is  $sl(c)$  and the corresponding chosen thresholds  $sl_{P0.01} = 0^\circ$  and  $sl_{P0.99} = 7.5^\circ$  (arbitrary choice). Then, with corresponding  $k_{el}$  and  $k_{sl}$  from equation 3.32, the penalties for terrain elevation and slope are calculated as

$$P_{el}(c) = \frac{1}{1 + \exp(-k_{el}(el(c) - \frac{el_{P0.01} + el_{P0.99}}{2}))} \quad (3.36)$$

$$P_{sl}(c) = \frac{1}{1 + \exp(-k_{sl}(sl(c) - \frac{sl_{P0.01} + sl_{P0.99}}{2}))} \quad (3.37)$$

The (combined) geographical penalty  $P_G$  for a cell  $c$  is simply the average of  $P_{el}$  and  $P_{sl}$ :

$$P_G(c) = (P_{el}(c) + P_{sl}(c)) / 2 \quad (3.38)$$

Figure 3.9 shows the geographic penalty,  $P_G$ , which is the same for all agents and constant over time.

**Population density.** Agents also avoid moving to locations with a large population density. While different agents share the same resources and, thus, interact with the same environment, their actions and moving decisions are independent from each other. However, by making locations with high population density unfavourable, the population penalty introduces an indirect agent-agent interaction. I define the population density of a cell as the population density within the farming radius of cell  $\tilde{c}$ , i.e.  $C_F(\tilde{c})$ .

$$pd(\tilde{c}) = \frac{\text{pop}|_{\hat{c} \in C_F(\tilde{c})}}{r_F^2 \pi} \quad (3.39)$$

The thresholds are chosen as

$$pd_{P0.01} = 0 \frac{\text{ppl}}{\text{km}^2} \quad (3.40)$$

and

$$pd_{P0.99} = 300 \frac{\text{ppl}}{\text{km}^2} \quad (3.41)$$

with estimated values of 262 and  $389 \frac{\text{ppl}}{\text{km}^2}$  on ‘prime agricultural land’ on Hawaii and Maui (Kirch, 2010; Puleston et al., 2017), which likely overestimate the maximum local densities on Easter Island (Puleston et al., 2017). Then, the (time dependent) population density penalty for one cell is

$$P_D(\tilde{c}) = \frac{1}{1 + \exp(-k_D(pd(\tilde{c}) - \frac{pd_{P0.01} + pd_{P0.99}}{2}))} \quad (3.42)$$

with the corresponding  $k_D$  calculated from equation 3.32.

**Availability of Trees.** Scarcity of trees in the local surrounding of a specific location also penalises a possible settlement. The tree penalty  $P_T(\tilde{c})$  is determined via the evaluation variable  $tr(c)$ , the number of trees within  $C_T(\tilde{c})$ ,

$$tr(\hat{c}) = \sum_{\hat{c} \in C_T(\tilde{c})} T(\tilde{c}, t) . \quad (3.43)$$

A cell with large value of  $tr$  has a lower tree penalty. There is no intuitive threshold for having a negligible tree penalty,  $tr_{P0.01}$  (or optimal number of trees). Here, I choose this value as the tree number sufficient to fill the tree requirement for a population of very high density,  $pd = pd_{P0.99}$ , in the tree search radius,  $C_T(c_i(t))$ , with maximum tree preference  $T_{\text{Pref, max}}$  for roughly one generation ( $\sim 45$  yrs).

$$tr_{P0.01} = T_{\text{Pref, max}} \cdot T_{\text{Req, pP}} \cdot \left( pd_{P0.99} \cdot \frac{r_T^2}{r_F^2} \right) \text{ppl} \cdot 45 \text{ yrs} = 216 \cdot 10^3 \text{ trees} . \quad (3.44)$$

The threshold,  $tr_{P0.99}$ , is chosen as the tree number required to keep the current agent's population at a happiness level of at least  $h_i(t) = H_{equ}$  for the next year:

$$tr_{P0.99,i} = T_{Pref,i}(t) \cdot T_{Req,pP} \cdot pop_i(t) \cdot H_{equ}, \quad (3.45)$$

which is typically between 10 – 100 trees depending on the properties of agent  $i$ . On top of the logistic penalty dependency, I further enforce a necessary condition of tree availability at  $tr_{P0.99}$ : A cell  $\tilde{c}$  is only considered as viable settlement location if the number of trees at least fulfils  $tr(\tilde{c}) \stackrel{!}{\geq} tr_{P0.99}$ . In total,

$$P_{T,i}(\tilde{c}) = \begin{cases} \infty & \text{if } tr(\tilde{c}) < tr_{P0.99} \\ \frac{1}{1 + \exp(-k_{tr}(tr(\tilde{c}) - \frac{tr_{P0.01} + tr_{P0.99}}{2}))} & \text{else} \end{cases} \quad (3.46)$$

**Availability of Farming Land.** Finally, also availability of farming sites influences the agent's moving decision. The penalty for farming, here, depends on two evaluation variables: The total available farming potential  $F_{tot}(\tilde{c})$  and the available farming potential from non-eroded, well-suited cells only,  $F_{well}(\tilde{c})$ . The penalties for both variables are calculated separately and then averaged. The total available farming potential is simply a summation of all productivity indices of arable, unoccupied sites (number of acres within a cell) within  $C_F(\tilde{c})$ .

$$F_{tot}(\tilde{c}) = \sum_{\hat{c} \in C_F(\tilde{c})} F_{PI}(\hat{c}) \cdot (A_{acres}(\hat{c}) - \mathbf{A}_F(\hat{c}, t)), \quad (3.47)$$

where  $A_{acres}(c)$  is the number of acres and  $\mathbf{A}_F(c, t)$  is again the number of occupied sites (and, therefore, unavailable to new agents) in cell  $c$ . Similarly, the farming potential for well-suited cells only is

$$F_{well}(\tilde{c}) = \sum_{\hat{c} \in C_F(\tilde{c}) \cup F_{PI}(\hat{c})=1} F_{PI}(\hat{c}) \cdot (A_{acres}(\hat{c}) - \mathbf{A}_F(\hat{c}, t)). \quad (3.48)$$

$F_{well}$  is an important consideration for agents as it makes cells more favourable, if the farming products can be obtained from a few well-suited rather than a larger number of poorly suited sites, which implies a larger workload. The threshold for an optimal location w.r.t. farming is the maximum possible land needed to be farmed by an agent with 42 individuals.

$$\begin{aligned} F_{well,P0.01} &= F_{tot,P0.01} = (1 - T_{pref,min}) \cdot F_{Req,pP} \cdot 42 \text{ ppl} \\ &= \begin{cases} 16.8 \text{ acres (with } F_{PI}(c) = 1 \text{) for high N fixation scenario} \\ 57.1 \text{ acres (with } F_{PI}(c) = 1 \text{) for low N fixation scenario} \end{cases} \end{aligned} \quad (3.49)$$

The threshold for penalty  $P_F(c) = 0.99$  is the agent's current farming requirement sufficient to obtain a happiness index of  $h_i(t) = H_{equ}$ , i.e.

$$F_{\text{well, P0.99, } i} = F_{\text{tot, P0.99}} = (1 - T_{\text{pref, } i}(t)) \cdot F_{\text{Req, pP}} \cdot \text{pop}_i(t) \cdot H_{equ}, \quad (3.50)$$

which depends on the tree preference and population size and is typically between 1 and 12 acres (with  $F_{PI}(c) = 1$ ) for the high N fixation scenario. Equivalent to the tree penalty  $P_T$ , a necessary condition for moving to a cell is enforced: A cell  $\tilde{c}$  is only considered as viable settlement location if the total farming potential at least fulfills  $F_{\text{tot}}(\tilde{c}) \stackrel{!}{\geq} F_{\text{tot, P0.99}}$ . Then, the total penalty is

$$P_{F, i}(\tilde{c}) = \begin{cases} \infty & \text{if } F_{\text{tot}} < F_{\text{tot, P0.99}} \\ \frac{0.5}{1+\exp(-k_F(F_{\text{well}}(c)-F_{P0.5}))} + \frac{0.5}{1+\exp(-k_F(F_{\text{tot}}(c)-F_{P0.5}))} & \text{else} \end{cases} \quad (3.51)$$

with  $F_{P0.5} = \frac{F_{P0.01}+F_{P0.99}}{2}$  and the parameter  $k_F$  from equation 3.32. In summary, the farming penalty is smallest for those cells surrounded by a lot of well-suited, available sites. The penalty is large for those cells surrounded by few available, arable sites in general and few available, well-suited sites in particular. At Anakena Beach, where open-sea fishing is allowed and, therefore, farming not required (if the external restriction  $N_{\text{Fisher}}(t) < N_{\text{Fisher, Max}}$  holds), I set the ‘farming’ penalty to a negative value to encourage agents to move there:

$$P_{F, i}(\hat{c}) = -1 \quad \forall \hat{c} \in C_F(c_{\text{Anakena}}) \text{ if } N_{\text{Fisher}}(t) < N_{\text{Fisher, Max}} \quad (3.52)$$

**From Penalties to Probability to New Location.** The resulting penalties for a cell  $\tilde{c}$  in  $C_M(c_i(t))$  from all categories are linearly combined to obtain a total penalty, which is then converted to a discrete probability  $Pr(\tilde{c})$  of moving to this cell. With (normed) weights  $\vec{\alpha}$  (and the agent's tree preference  $T_{\text{Pref, } i}(t)$ ):

$$\vec{\alpha}_i(t) = \left( \alpha_G, \alpha_W, \alpha_D, \frac{T_{\text{Pref, } i}(t)}{\eta_i(t)} \cdot \alpha_T, \frac{(1 - T_{\text{Pref, } i}(t))}{\eta_i(t)} \alpha_F \right) \quad (3.53)$$

where  $\eta_i(t) = \frac{\alpha_T T_{\text{Pref, } i} + \alpha_F (1 - T_{\text{Pref, } i})}{\alpha_T + \alpha_F}$  is a normalisation factor to ensure that,  $\frac{T_{\text{Pref, } i}(t)}{\eta_i(t)} \cdot \alpha_T + \frac{(1 - T_{\text{Pref, } i}(t))}{\eta_i(t)} \cdot \alpha_F = \alpha_T + \alpha_F$  and, therefore,  $\|\vec{\alpha}_i(t)\| = 1$ . The total penalty is:

$$P_{\text{tot, } i}(\tilde{c}, t) = \begin{cases} \infty & \text{if } \tilde{c} \notin C_M(c_i(t)) \\ \langle \vec{\alpha}_i(t), \vec{P}(\tilde{c}) \rangle & \text{else} \end{cases} \quad (3.54)$$

Table 3.1: The evaluation variable,  $x$ , and chosen thresholds,  $x_{P0.01}$  and  $x_{P0.99}$ . Inserting these into the logistic function  $P_X(x)$  (equation 3.31) gives the penalties in each category  $X$ :  $P_G$  for geography,  $P_W$  for freshwater proximity,  $P_D$  for population density,  $P_T$  for tree availability,  $P_F$  for farming land availability. Note, that  $x_{P0.99}$  for category  $T$  and  $F$ , which represent also the necessary minimum amount of resources required, depend on the specific agent's properties (denoted by \*). For the farming penalty, the thresholds are calculated for the high Nitrogen fixation scenario here. For  $P_G$  and  $P_F$ , which have two elevation variables, the mean of the sub penalties gives the corresponding category penalty (see Sketch in Figure 3.10).

$X$	$x$	Description	$x_{P0.01}$	$x_{P0.99}$	Unit	Necessary Condition
W	$w$	Area weighted distance of cell to lake	$\frac{(0.5 \text{ km})^2}{r_{\text{Raraku}}^2 \pi}$	$\frac{(5 \text{ km})^2}{r_{\text{Raraku}}^2 \pi}$	—	
G	$el$	Elevation	0	300	m	
	$sl$	Slope	0	7.5	°	
D	$pd$	Population density within $r_F$	0	300	$\frac{\text{ppl}}{\text{km}^2}$	
T	$tr$	Number of trees within $r_T$	$216 \cdot 10^3$	$\sim 10 - 100 *$	Trees	$tr \geq tr_{P0.99}$
F	$F_{\text{tot}}$	Total possible farming produce within $r_F$	16.8	$\sim 1 - 12 *$	acres	$F_{\text{tot}} \geq F_{\text{tot}, P0.99}$
	$F_{\text{well}}$	Possible farming produce of well-suited sites within $r_F$	16.8	$\sim 1 - 12 *$	acres	

with  $\vec{P} = (P_G, P_W, P_D, P_{T,i}, P_{F,i})$ . Finally, the probability is

$$Pr(\tilde{c}) = \frac{1}{N} \cdot \exp(-\gamma \cdot P_{\text{tot},i}(\tilde{c}, t)) \quad (3.55)$$

where  $N$  is a normalisation and  $\gamma$  is a dimensionless scaling factor, which represents the agent's tendency to actually follow the penalty evaluation. By increasing  $\gamma$ , the agent's move more likely to spaces with higher probability (low total penalty). E.g. for  $\gamma \rightarrow \infty$ , agents have perfect knowledge of the island's properties and move to the optimal cell with minimal penalty, i.e. the decision making is a fully deterministic optimisation process<sup>19</sup>. On the other hand,  $\gamma = 0$  implies that agents move to any new location without consideration of the associated penalties. By choosing  $\gamma$  large, but finite, I set the agents up to make individualistic, semi-rational choices when moving, but include stochasticity (e.g. due to imperfect knowledge) in the decision. An agent moves to a site based on individual assessment. However, multiple agents share the same local environment and, thus, can quickly change the penalties of a location (e.g. through deforestation). Hence, a low penalty at a certain time, does not imply favourable conditions for the future.

Having selected a new cell, the agent chooses a location within this cell with uniform probability<sup>20</sup>. The total procedure of calculating the probability is sketched in Figure 3.10.

**Computation Time of the Moving Process.** The decision making process when an agent moves is the bottleneck w.r.t. computation time in the ABM. A single evaluation process scales quartic with the grid resolution  $\delta_{x,y}$ , i.e.  $\mathcal{O}(\delta_{x,y}^4)$ : The overall number of cells to consider,  $N_c$ , increases quadratic with  $\delta_{x,y}$  and the evaluation of penalties (e.g. summing up trees from cells in  $C_T(\tilde{c})$ ) for evaluation of a single cell also scales quadratic with the grid resolution. In order to increase efficiency, I use dot products and distance matrix computation from the python packages *numpy*<sup>21</sup> and *scipy*<sup>22</sup>, both implemented in C++.

---

<sup>19</sup>Proof: Consider the relation between  $Pr(c_{\min})$ , where  $c_{\min}$  denotes the cell with the minimal penalty  $P_{\text{tot},\min}$ , and  $Pr(c)$  for all cells  $c$ . Then,  $Pr(c_{\min})/Pr(c) = \exp(-\gamma P_{\text{tot},\min})/\exp(-\gamma P_{\text{tot}}(c)) = \exp(-\gamma \cdot (P_{\text{tot},\min} - P_{\text{tot}}(c)))$ . For  $\gamma \rightarrow \infty$  this converges to  $\delta_{c=c_{\min}}$ .

<sup>20</sup>Note, that by choosing a location within this cell, the actual availability of arable, free land and/or trees, might deviate slightly from the calculation of the cell's penalty, as the agent's new location (and therefore the definition of the local environment) is not the midpoint as used for the calculation in the moving process. This accuracy error decreases with a higher discretisation resolution.

<sup>21</sup>Olliphant (2006)

<sup>22</sup>Virtanen et al. (2020)

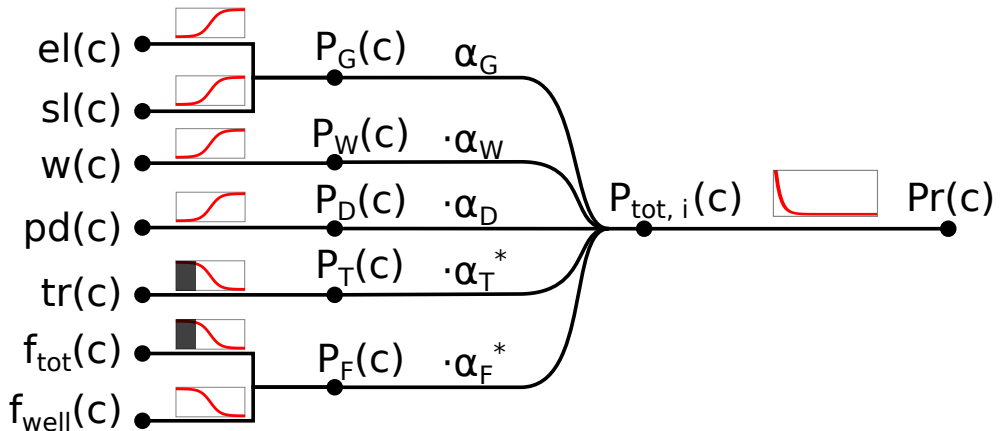


Figure 3.10: A sketch of the calculation of the probability for agent  $i$  to relocate its settlement to cell  $c$ : The category penalties ( $P_G$  for geography,  $P_W$  for freshwater proximity,  $P_D$  for population density,  $P_T$  for tree availability,  $P_F$  for farming land availability) are calculated via one or two characteristic evaluation variables described in the main text assuming a logistic functional dependence (red curves). If two evaluation criteria are considered for one category, the resulting sub-penalties are averaged (crossings for  $P_G$  and  $P_F$ ). For  $P_T$  and  $P_F$ , cells that do not have the minimum required resource availability are excluded (grey boxes). The total penalty for cell  $c$ ,  $P_{\text{total}, i}(c)$  is then a linear superposition of all category penalties (with the weights  $\alpha_T^*$  and  $\alpha_F^*$  adjusted according to the tree preference  $T_{\text{Pref}, i}(t)$  in equation 3.53). The final probability for a cell  $c$  is derived as  $Pr(c) \sim e^{-\gamma \cdot P_{\text{tot}, i}(c)}$  (red line in the right part), with scaling factor  $\gamma$ .

In an alternative implementation, one could adjust penalties (or characteristic variables) immediately when the agents interact with the environment, which would scale as  $\mathcal{O}(\delta_{x,y}^2 \cdot N_{\text{agents}}(t) \cdot N_{\text{timesteps}})$ . However, since the resolution does not have to be small for the purpose of this study, the first implementation is not necessarily slower.

Table 3.2: Choices of parameters for the standard configuration run and sensitivity analysis.

Parameter	Value	Unit	Reference	Description	Sensitivity Tests
$t_{\text{arrival}}$	800	A.D.	Bahn and Flenley (2017)	Start of simulation	–
$\text{pop}_{\text{arrival}}$	40	ppl	Brander and Taylor (1998)	Population at $t_{\text{arrival}}$	–
$F_{\text{Req, pP}}$	0.5	$\frac{\text{acres}}{\text{person}}$	Puleston et al. (2017)	Required (optimal) farming acres per person (high fixation)	1.7 (low fixation)
$F_{\text{PI, well}}$	0.8	–	Louwagie, Stevenson, and Langohr (2006)	Productivity index of well-suited cell	–
$F_{\text{PI, eroded}}$	0.5	–	–	Productivity index of eroded, well-suited cell	–
$F_{\text{PI, poor}}$	0.1	–	Louwagie, Stevenson, and Langohr (2006)	Productivity index of poorly suited cell	–
$T_{\text{Req, pP}}$	5	$\frac{\text{Trees}}{\text{person}\cdot\text{yr}}$	Brandt and Merico (2015)	Required trees per person per year	10
$T_{\text{Pref, min}}$	0.2	–	–	Minimum tree preference of an Agent	–
$T_{\text{Pref, max}}$	0.8	–	–	Maximum tree preference of an Agent	–
$T_{\text{Pref, min}} _{\text{fisher}}$	0.5	–	–	Minimum Tree preference of a fisher agent	–
$N_{\text{Fisher, Max}}$	10	–	–	Maximum number of fisher agents	–
$r_F$	1	km	–	Searching radius for farming site	0.5 and 2
$r_T$	2	km	–	Searching radius for trees	1 and 4
$f_{\text{Tree Pref}}$	linear	–	–	Strategy for adapting the tree preference to local environmental change	delayed, faster logistic

$T(t_{\text{arrival}})$	$16 \cdot 10^6$	Trees	Mieth and Bork (2015) Bahn and Flenley (2017)	Total number of trees before arrival Uniform density for $el(c) < 450\text{m}$ , $sl(c) < 10^\circ$	—
Tree Pattern	—	—	Hunt (2007); Bahn and Flenley (2017)	Max (logistic) growth rate of trees ( $0 \hat{=} \text{'without'}$ )	‘with’ <sup>a</sup>
$g_T$	0	%/yr	Rull (2020)	Drying of Rano Raraku	—
Droughts	800 – 1200 & 1570 – 1720	A.D.	Lee and Tuljapurkar (2008) Puleston et al. (2017)	Scale of Gamma CDF describing an agent’s growth rate $g(H_i(t))$	—
$g(H_i(t))$ (scale)	0.1	—	Bahn and Flenley (2017)	Happiness at which $g(H_{\text{equ}}) = 1$ <sup>b</sup>	0.84
$H_{\text{equ}}$	0.688	—		Initial growth rate (with unlimited resources)	—
$g(H_i(t) = 1)$	0.7	%/yr			
$pop_{\min}$	6	ppl	—	Minimum population of a household	—
$pop_{\max, \text{mean}}$ ( $pop_{\max, \text{std}}$ )	42 (3)	ppl	—	Gaussian splitting probability of a large household	—
$pop_{\text{split}}$	12	ppl	—	Population size of a new agent after splitting	—
$r_M$	5	km	—	Searching radius for a new location (if $\text{pop}(t) > 5000$ )	—
$x_{P0.01}/x_{P0.99}$	...	...	...	see Table 3.1	—
$\vec{\alpha}$	$\alpha_x = 0.2 \forall x$	—	—	Weights for penalty categories in moving decision	$\alpha_{T,F} = 0.5$
$\gamma$	20	—	—	Scaling factor for probability depending on the total penalty	0, 1000

<sup>a</sup> With tree regrowth:  $g_T = 5\%/\text{yr}$ , and ‘pop up’ on barren cells (0.5% of carrying cap after 10 years).

<sup>b</sup> This determines the shape of the Gamma CDF describing the growth rate of the human population,  $g(H_i(t))$ : For  $H_{\text{equ}} = 0.688$ ,  $shape = 1.95$ , for  $H_{\text{equ}} = 0.84$ ,  $shape = 3$

# Chapter 4

## Results and Discussion

### 4.1 A Standard Configuration Run

**Overview of the Results.** The standard configuration run results of the ABM presented in Section 3 are produced with parameters presented in Table 3.2. Figure 4.1 presents snapshots of a simulation showing the spatial pattern of trees, farmed sites, and agents (with their tree preferences) at different times. In the supplementary material, I provide a link to an animated Figure showing the evolution of these spatial patterns over time. Since multiple processes in the model are stochastic, each run with a specific seed is a unique realisation. In order to obtain statistically valid aggregate results, I use an ensemble of 15 runs for all experiments. Adding more runs (e.g. 20 or 25) does not significantly change the coefficient of variation for the ensemble over time (see Figure B.1). The mean and standard deviation of the aggregated variables of this ensemble and their change over time is shown in Figure 4.2. The uncertainty in the ensemble runs results from slight differences in the timing of the dynamics due to different realisations of the discrete, stochastic population growth process (see also Figure A.1). Hence, the peaks of the population sizes of single runs are at a similar level but slightly shifted in time. However, due to this shift the resulting ensemble mean (thick line in Figure 4.2) slightly underestimates the peak population size.

**The first phase: Initial Growth.** In the beginning of the simulation, two agents with 20 individuals each settle at Anakena Beach (in the North in Figure 1.1). The local tree density is at the carrying capacity (in total  $16 \cdot 10^6$  trees) and, thus, the agents' tree preference is high (blue colour in Figure 4.1). In the first phase of the simulated time period, the agents' population

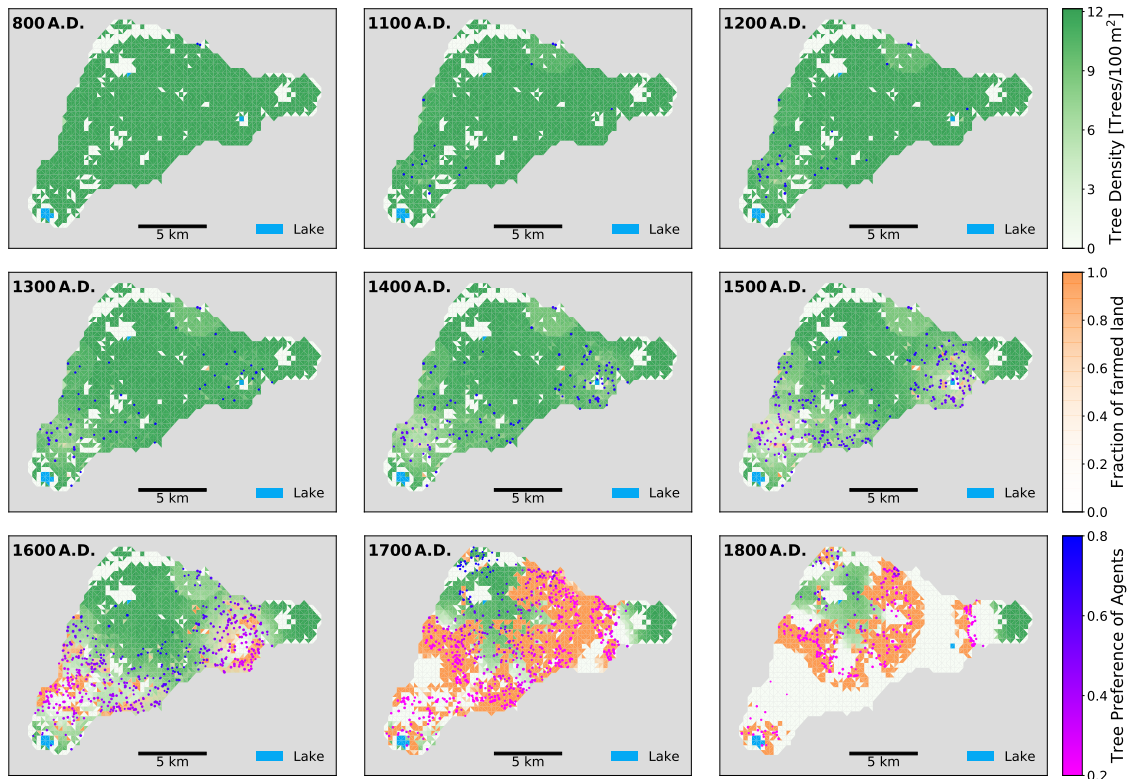


Figure 4.1: Spatial patterns produced by the ABM in the standard run configuration at nine different times (comparable to Figure 9 in Rull, 2020). The map shows the tree density in green and the fraction of farmed land in orange. Agents are represented by dots with a colour corresponding to their tree preference and size corresponding to their population size. They settle on the island and interact with the environment by cutting trees and turning arable land into farmed sites.

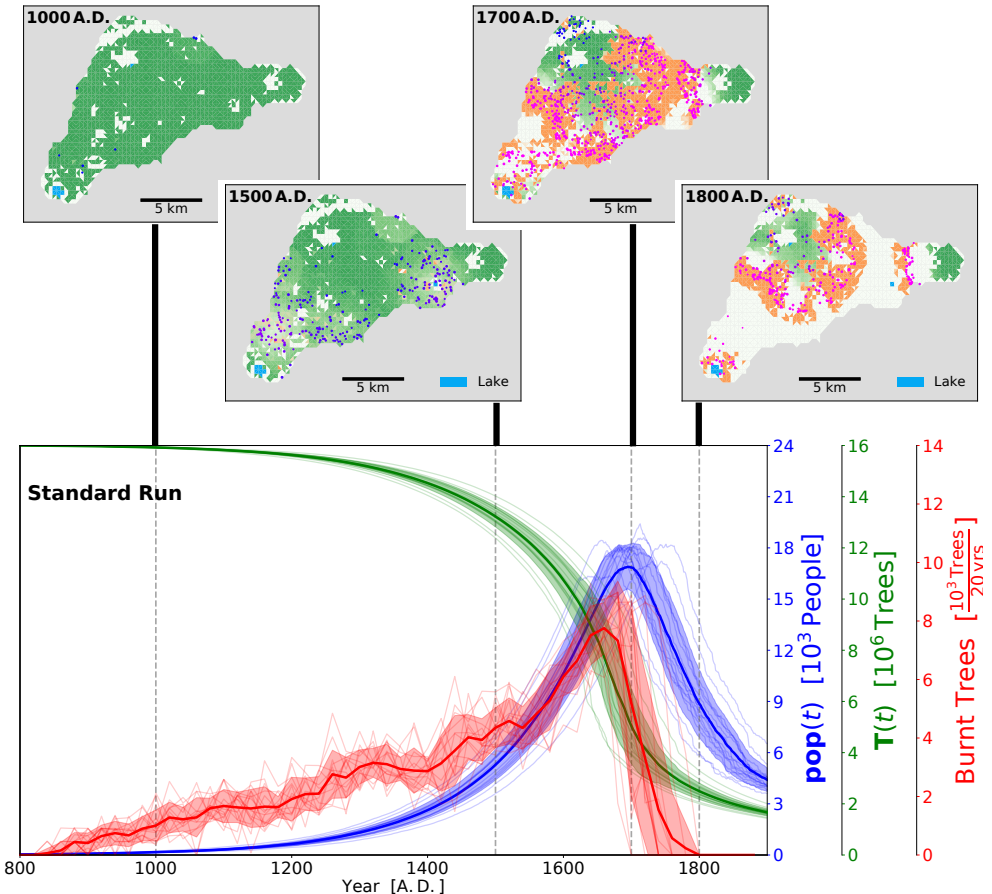


Figure 4.2: Dynamics of aggregate population size, trees, and burnt trees in the standard run configuration. 15 different realisations (thin lines) are used to obtain the ensemble means (thick lines) and standard deviations (shaded areas). The number of burnt trees is presented in bins of 20 years, as its variation is strong. The maps above show the spatial distribution of trees, farming and agent settlements with their tree preferences for one of these realisations (with the same colour coding as in Figure 4.1).

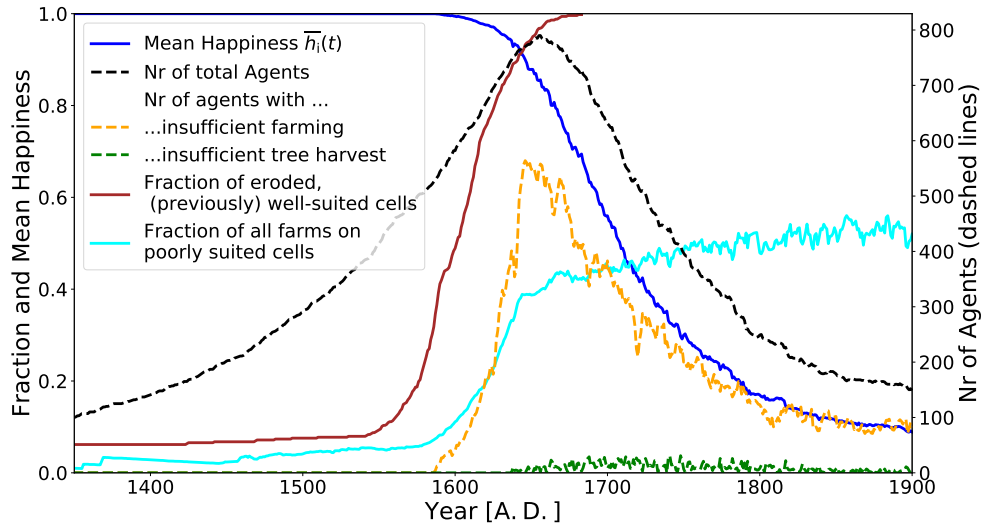


Figure 4.3: Indicators of the change from net growth to net decline in population dynamics for one single realisation in the standard run configuration. Dashed lines correspond to the y-axis on the right representing absolute number of agents. The blue line shows the mean happiness index of all agents. The black, dashed line shows the total number of agents. The number of agents that lack either sufficient land for farming or trees are shown in yellow and green, respectively. The brown line shows the fraction of cells (previously classified as well-suited for farming) with erosion due to complete deforestation. The cyan line shows the fraction of farming sites on poorly suited sites.

size grows at a constant maximum growth rate, because trees and arable land are both abundant. Consequently, the number of agents increases and new agents start to colonise the rest of the island. Until the end of the first drought period in 1200 A.D., new agents tend to settle in the arable, coastal region South/South East of the island close to the major freshwater source Rano Kau. After 1200 A.D., also the region around Rano Raraku (in the West), now providing an alternative, low elevation freshwater source, is settled at rapid pace. Agents linearly adapt their tree preference to the slow environmental change and, thus, intensify farming activity. As Figure 4.2 shows, the amount of burnt trees to clear land for agriculture also increases linearly in this phase.

**The second phase: Acceleration.** The second phase of the dynamics is characterised by accelerating, non-linear feedbacks as shown by several indicators (Figure 4.3). In a self-enhancing loop, population growth in the settlement centres leads to an intensification of deforestation, a consequent decrease of the agents' tree preferences, increase of farming requirements, more acquisition of farming sites (therefore, more burnt trees) and, thus, more in-

tense deforestation. Simultaneously, erosion accelerates the deforestation as the farming productivity of occupied land decreases and more land needs to be acquired. The portion of eroded, previously well-suited cells jumps from less than 10% of all well-suited sites in 1600 A.D. to 100% by 1700 A.D. (brown curve in Figure 4.3). Consequently, the amount of trees burnt for clearing land rises sharply. In total, this acceleration of local resource use, leads to an abandonment of the previously used well-suited locations (constituting nearly 100% of all farming activity in 1650 A.D.) and to the colonisation of mostly poorly suited, interior, upland areas (accounting for 40% in 1700 A.D., cyan line in Figure 4.3).

**The third phase: Population Decrease.** The third phase is characterised by a population decline and a substantial shift in the settlement patterns. While in 1700 A.D. more than half of the agents experience some minor shortage in farming products (yellow curve in Figure 4.3), the loss of the trees, experienced by a few agents each year (green line in Figure 4.3) triggers an exponential decline in averaged happiness,  $\bar{h}_i(t)$ , just after 1700 A.D. (blue line in Figure 4.3). This leads to a period of intense moving. Figure 4.4 shows examples of an agent's penalties while searching for a new settlement location. This phase marks the end of net exponential growth for the population, which peaks at around  $18 \cdot 10^3$  people around 1700 A.D.. Within a relative short time period of less than 50 years, the population starts to decrease exponentially with a growth rate of  $-0.5$  to  $-1\%$  (see Figure B.2 in the Appendix). The population decreases despite the fact that there are always both unoccupied farming sites and sufficient total number of trees on the island. However, since the harvest is confined to the local surrounding of an agent in a specific location, it typically lacks one or the other resource and at some point there are no suitable locations left that fulfil both resource requirements. Consequently, an agent's effective happiness,  $H_i(t)$  quickly drops to 0 and the overall population size decreases. As a result of the decreasing population size, the deforestation level slows down around 1750 A.D. at slightly less than 25% of the initial total number of trees. However, there is no stable coexistence of population and trees in this standard run configuration as tree regeneration is disabled and, hence, the agents rely on a non-renewable resource and, eventually, all agents vanish as it becomes exhausted.

**Outcomes Consistent with Ecocidal View.** The succession of events in the standard run configuration follows a boom and bust scenario consistent with the classical narrative of a Malthusian catastrophe driven by overexploitation

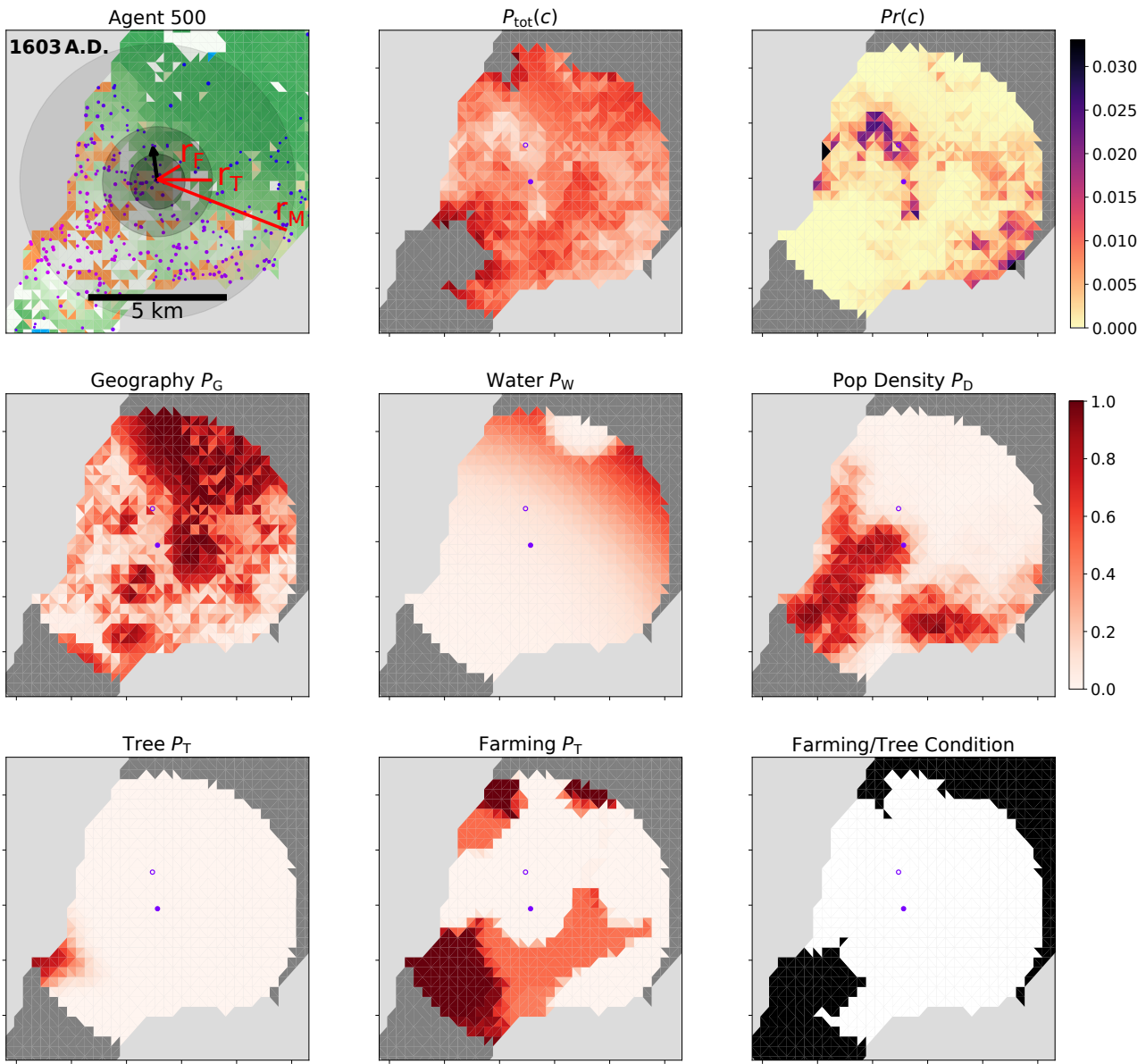


Figure 4.4: Decision making in the moving module of an agent at 1603 A.D. in the South Eastern portion of the island. Each panel shows the same region of interest with the location of the agent in the centre (filled dot) and the new location after the decision is made (unfilled dot). The upper left panel shows the agent in its current local environment, indicated by circles with the radii  $r_F$ ,  $r_T$ , and  $r_M$  (after the moving restriction). The upper middle panel shows the total penalty ( $\in [0, 1] \cup \infty$ ), and upper right the corresponding probability for the agent to move to each allowed cell. The remaining panels show the penalties in all categories ranging from 0 to 1. The lower right panel also shows the cells that are excluded from the search because they do not fulfil the necessary condition for tree and farming availability (black cells inside the  $r_M$  circle).

as theorised by Brander and Taylor (1998), Diamond (2011) and Bahn and Flenley (2017). This is not surprising as the agents are designed to maximise their personal population growth every year while they rely (in the standard run configuration) on a non-renewable resource (trees) and a limited, renewable resource (farming products). Furthermore, the arrival date and initial population growth are taken from the ecocidal narrative.

**Population Size is Maximised Myopically by Model Design.** In general, the population size reached with this model is at the upper range of most estimates reported in the literature (Bahn and Flenley, 2017). This is partly due to the fact, that there is no restriction on the amount of labour that agents can put into the resource acquisition. Also, the model does not include any social development or political institution e.g. to stabilise the population growth or harvest of natural resources via taboos. Further, I assume that except for the eventual erosion of all well-suited cells, arable land has a constant, entirely predictable crop output (which I assume constant even during drought periods). Land availability is, thus, the only constraint for agricultural production in this model configuration. Sustainability criteria concerning the resource availability (locally and island-wide) do not play a role in the agents' myopic, unabated population expansion as long as the resource situation allows it. In addition, agents do not plan ahead while harvesting e.g. trees could be cut first (e.g. for extracting the sugary sap) and then burned to clear land for farming in the following year as suggested by Mieth and Bork (2015). Only when resources become scarce, the population growth declines and turns negative. The pronounced consequent decrease in population size is, thus, inevitable as agents are determined to overexploit.

**The Spatial Component.** This modelling work investigates for the first time spatial component of the Easter Island settlement history emerging from the local harvest behaviour and moving decisions of autonomous agents. The results (in terms of tree densities and temporal and spatial distributions, Figure 4.1) show good agreement with a qualitative reconstruction of tree density obtained from charcoal and pollen data by Rull (2020) (Figures 7 and 9 in the cited literature). The spatial Easter Island settlement history produced by the model is also mostly consistent with a qualitative colonisation pattern suggested by Bahn and Flenley (2017) based on archaeological evidence. This qualitative pattern proposed by Bahn and Flenley (2017) is as follows. Settlement of some coastal regions, especially South East Coast near Rano Kau and Anakena Beach (800 to 1100 A.D.), settlement of the whole coast (1100 – 1425 A.D.,

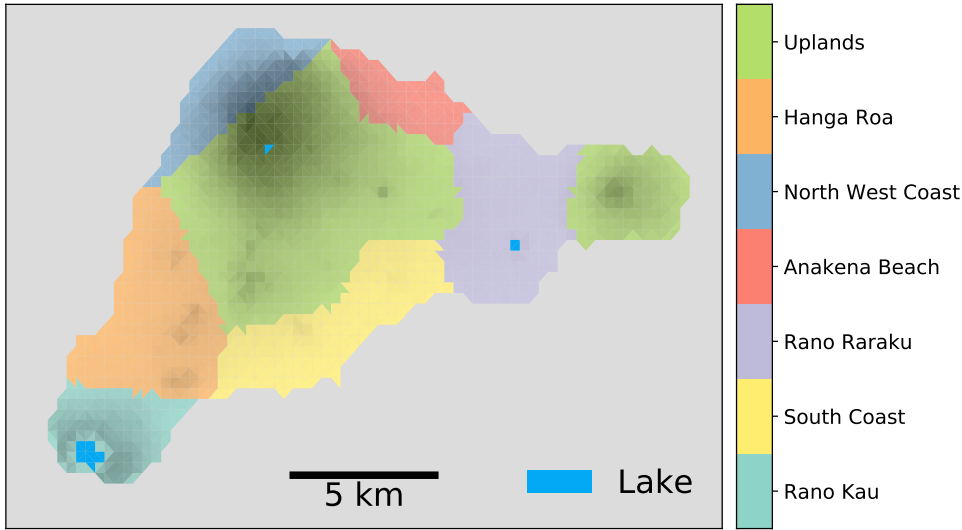


Figure 4.5: Division of the map into seven separate regions. The black shadow represents elevation.

with a rapid population increase in the South Coast around 1300 A.D.), a peak of the population size and farming activity (1425 – 1680 A.D.), and, finally, population reduction and remote fields abandoned<sup>1</sup> (1680 A.D. to the 18th century followed by European contact).

**Temporal Dynamics in Different Regions.** The model results suggest strong regional variation in the dynamics of the population as well as the deforestation as shown in Figure 4.1. To quantitatively analyse these different developments, I divide the island into seven different regions with specific geographical features (Figure 4.5): (1) the area around the crater lake Rano Kau, (2) the South Coast, (3) Rano Raraku, (4) Anakena Beach, (5) the steep North West Coast, (6) the fertile area covering today's main town, Hanga Roa, and (7) the upland area including Poike Peninsula. By choosing centre points of each region or several sub-regions on the map by hand, a region is defined by the cells allocated to the corresponding Voroni Diagram.

Figure 4.6 shows the results of the population in each region over time in the ensemble of 15 runs. Overall, the island shows diverse and heterogeneous population dynamics. Some regions, like Hanga Roa and the South Coast (with a little delay), show early extensive growth followed by a steep decline of the

<sup>1</sup>The results of the model presented in this thesis do not show such an abandonment of upland fields.

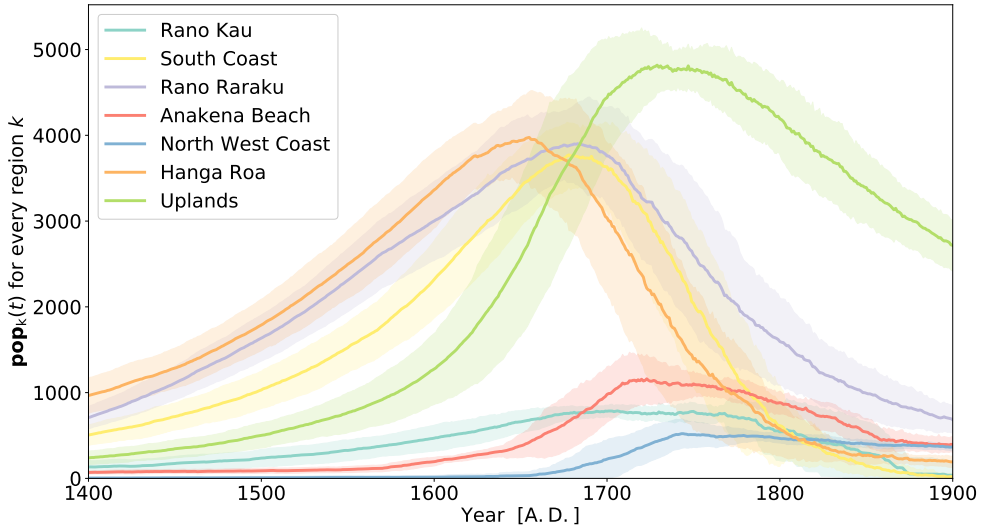


Figure 4.6: The population dynamics of each separate region defined in Figure 4.5 as an ensemble of 15 single realisations.

population. The population around Rano Raraku grows nearly linearly and then, as in the Uplands, declines less strongly after the peak. In some single realisations, this effect is more pronounced than in the ensemble mean. The small, less arable regions at Rano Kau, the North West Coast, or Anakena Beach, show some population growth following the abandonment of other, more favourable regions. The population size in these regions then either declines close to linearly or even remains at the same level for nearly 200 years. Given these strong variations between different regions, caution should be exercised when extrapolating results obtained from archaeological evidence in specific regions to the whole island. This modelling study, however, gives indications about the implications of these regional differences for the whole island.

## 4.2 Experiments and Sensitivity Analysis

### 4.2.1 Abundance of and Requirements for Resources

**Outcomes Consistent with Different Narratives.** The standard run configuration used in the Section 4.1 reproduces a boom and bust dynamics. However, the parameters in this configuration are debatable and this uncertainty lies at the heart of the contrasting views of Easter Island’s historical development. In particular, the (spatially varying) farming yields on Easter Island

soils (here expressed via  $F_{\text{Req, pP}}$  and, correspondingly,  $F_{\text{PI}}(c)$ ) are uncertain. Also,  $T_{\text{Req, pP}}$  is speculative and in fact probably highly heterogeneous between agents. These constant parameters,  $F_{\text{Req, pP}}$  and  $T_{\text{Req, pP}}$ , determine the amount of tree harvesting and farmland occupation and, thus, are crucial for the temporal development of the island's environment and the peak population size. In a series of experiments, I change these constants,  $F_{\text{Req, pP}}$  and  $T_{\text{Req, pP}}$ , and/or additionally allow tree regeneration. Figure 4.7 shows four different scenarios with strongly varying results.

- The upper left panel shows the standard run configuration, which considers the high Nitrogen fixation scenario of Puleston et al. (2017) for  $F_{\text{Req, pP}}$  and without tree regeneration.
- The upper right panel, shows the case with low Nitrogen fixation by Puleston et al. (2017), i.e. agents have a higher requirement of farmed land per person. Population size (blue) peaks earlier and at a smaller number (ca. 6000 people) and the consequent decrease is slower with a rate close to  $-0.2\%/\text{yr}$ . The amount of burnt trees (red) especially in the first phase with constant population growth rate is higher in this scenario, because more arable land needs to be occupied by the agents.
- In the corresponding bottom panels, tree regeneration is enabled with parameters set as in Table 3.2. For both cases with tree regrowth (lower panels), a heterogeneous pattern of agents with different tree preferences emerges with some areas characterised by agents with maximum, some with minimum tree preference (not shown here).
  - In the lower left panel, with high Nitrogen fixation, a population of nearly  $24 \cdot 10^3$  individuals is reached at a later time than in the standard setting. After that peak, the population size then declines slowly until an equilibrium between tree renewal and tree cutting is reached with all arable sites being occupied after 1700 A.D.. There are two temporarily separated peaks in the amount of burnt trees around 1300 A.D. and 1650 A.D..
  - In the lower right panel, with low Nitrogen fixation, population peaks at a similar level and time compared to the case without tree regrowth. Here, however, the population size remains constant roughly at this peak level with all arable sites being occupied before 1600 A.D..

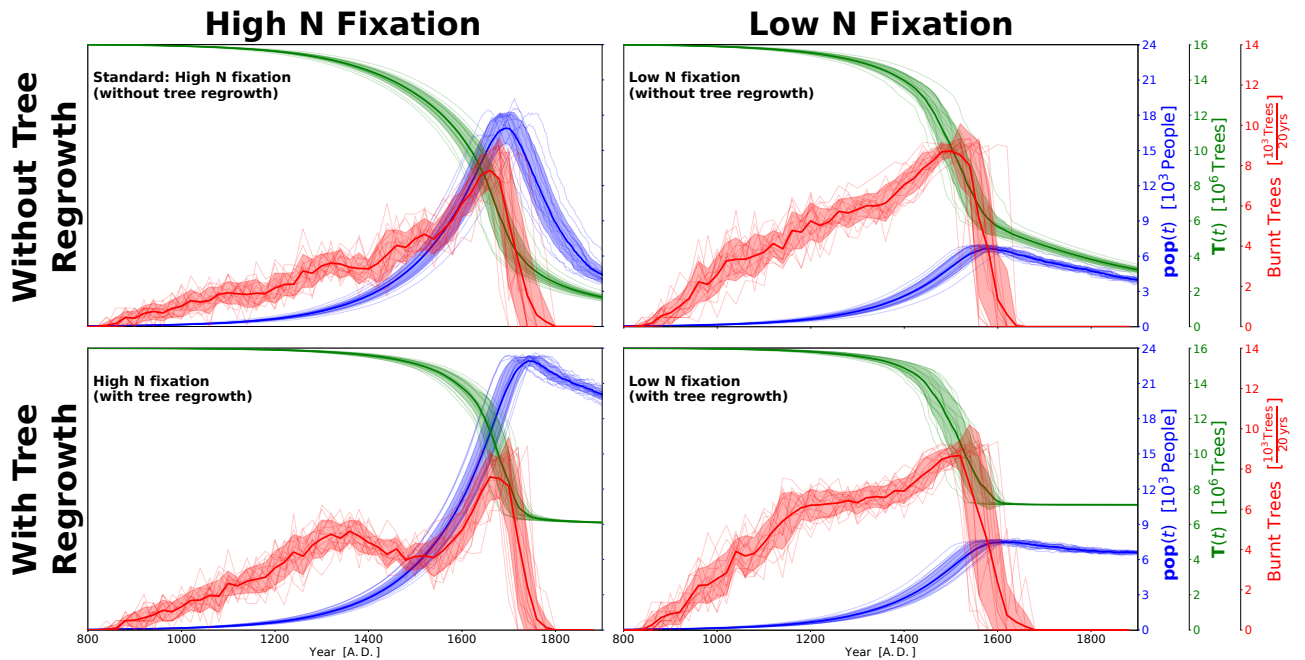


Figure 4.7: Dynamics of aggregate population size, trees, and burnt trees for four different parameter settings: The high or low N fixation scenario determining the amount of arable land required per person in combination with disabled/enabled tree regrowth. All panels show mean dynamics obtained from an ensemble of 15 runs.

A further experiment (not shown) with increased tree requirement per person  $T_{\text{Req, pP}}(t) = 10 \frac{\text{Trees}}{\text{yr}\cdot\text{person}}$  yields a similar boom and bust as in the standard run configuration but the population size peaks earlier and, thus, at a lower peak level ( $\sim 13000$ ), and with more intense deforestation.

The population dynamics obtained from these different scenarios varying only in two or three parameters reflect the contrasting storylines about the historic population dynamics of Easter Island currently present in the scientific debate. In particular, the low Nitrogen fixation scenario<sup>2</sup> resulting in constant or only slowly decreasing population size decline corresponds to the genocidal (Hunt, 2007) or slow-demise (Brandt and Merico, 2015) views.

### 4.2.2 Resource Search Radii

**Aggregate Dynamics.** In Figure 4.8, I present a sensitivity analysis of the resource search radii, which are increased or decreased by a factor of 2 (left) or 1/2 (right), respectively, compared to the standard run configuration. For

<sup>2</sup>consistent with Hunt (2007)'s assumption of low quality soil

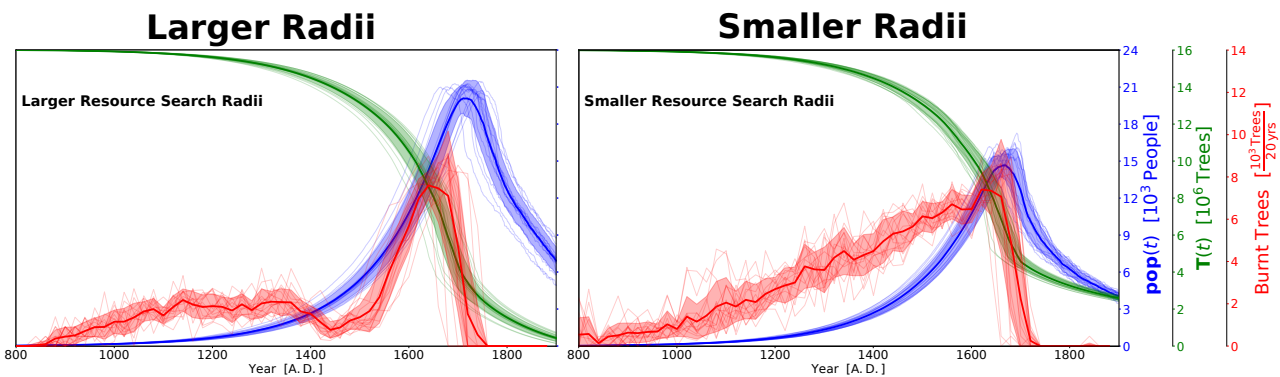


Figure 4.8: Dynamics of aggregate variables (as before) for variation of the resource search radii: The left panel shows runs with factor 2 larger radii:  $r_T = 4$  km and  $r_F = 2$  km; The right panel with factor 1/2 smaller radii:  $r_T = 1$  km and  $r_F = 0.5$  km. While changing the resource search radii does not change resource requirements or abundance, all aggregate variables depend strongly on this choice.

larger radius the peak population size increases, deforestation intensifies and the amount of burnt trees remains low for a long time but rises steeply around 1600 A.D.. At smaller radius, the peak population size strongly decreases, deforestation is less intense, and burning of trees increases linearly until a cut-off. Variation of the resource search radius has a non-trivial influence on the aggregate dynamics. While a larger (or smaller) radius increases (or decreases) an agent's access to resources at its current location, it does not change the amount of available resources on the island or required resources by the agents. As Figure 4.8 shows, the differences of the results between those scenarios are significant. Even though the carrying capacity of the island with respect to the amount of resources is the same, the agent's harvest behaviour is restricted by its local context and, hence, this lack of either available arable land or trees in the local environment changes the shape of the aggregate dynamics.

**Social Structure** It is clear that the social and economic structure of the Easter Island population is much more complex than the independent, small households of a few dozen people acting independently and myopically as assumed in this model. E.g. Diamond (2011) describes the existence of roughly a dozen clans or chiefdoms. Puleston et al. (2017) consider an economic structure formed by elite and working classes. Also, there is clear evidence of exchange of goods between households and clans or chiefdoms, e.g. fish, stone tools or the Moai. Such social structures would also allow for imposing taboos on the harvest of natural resources and increase the sustainability, although with limited effectiveness according to some researchers (Good and Reuveny,

2006). All of these complex, institutional structures based on agent-agent interactions are not considered here, but each agent farms and deforests individually. Including such social and political institutions would smooth the impacts of changing the resource search radii (or the local confinement of agents) and, thus, might lead to different population dynamics.

**Outlook: Clusters and Chiefdoms.** The model presented here can be extended to show the emergence of clustered agents that cooperatively harvest resources. E.g. Figure B.3 shows the centre points of 7 clusters obtained by k-Means clustering of the three dimensional space spanned by the agent's position and tree preference trait,  $(x_i, y_i, T_{\text{Pref}, i}) (t)$  for agent  $i$ , in one specific year, 1650 A.D. using the python packages *scikit-learn*<sup>3</sup> and *yellowbrick*<sup>4</sup>. For all tested years (between 1200 and 1900 A.D.) a number of 7 to 9 clusters are optimal according to the elbow method<sup>5</sup>. While this analysis is very preliminary, clustering might open up the possibility of including stronger links within clusters of agents that tend to move towards each other (e.g. negative population density penalty), harvest cooperatively, and increase the resource search radius with the cluster size. One could even think of including a trading module between clusters (as in Heckbert, 2013). Future research with this model could investigate more complex economic and social structures and, thereby, overcome one of the major weakness, the self-centred, non-cooperative harvest behaviour of the agents considered here.

### 4.2.3 Population Growth

**Aggregate Dynamics.** I test the stability of the model results to a less resilient demography. By increasing the shape parameter of  $g(H_i)(t)$  an agent's population size exhibits a steeper and earlier decline as  $H_i(t)$  decreases. However, in the standard run configuration, happiness of the agents decreases rapidly from 1 to 0 typically close to the peak population size and an agent can not find a place sufficient for meeting both resource requirements. Hence, the results are nearly independent from this variation of the population growth model<sup>6</sup>. However, for the scenario with tree regrowth the stable equilibrium between

---

<sup>3</sup>Pedregosa et al. (2011)

<sup>4</sup>Bengfort et al. (2018)

<sup>5</sup>The elbow is a heuristic to estimate the number of clusters: Running the k-Means algorithm with more clusters only linearly decreases the distortion, i.e. the sum of the squared distances of an agents 3D state to the cluster centres.

<sup>6</sup>In this simulation the ensemble net population decrease sets in only 10 years prior to the standard case and at the same peak level.

tree regrowth and tree cutting can sustain fewer individuals (roughly 2000 less, not shown) for this less resilient population scenario and its higher equilibrium happiness,  $H_{\text{equ}}$ .

**Oversimplified Population Growth.** The population dynamics in this ABM is subject to several limitations. The use of the food-limited demography model from Puleston et al. (2017) is strongly simplified here. E.g. I use a different notion of Puleston et al. (2017)'s food ratio, which I express via the effective happiness  $H_i(t)$  reflecting the (smoothed) success in cutting trees and farming. Also the distinction between survival and fertility rate especially given their age-dependency is entirely neglected. One major problem with the assumed population dynamics in this model is the fast decrease of effective happiness when the resource, trees, becomes scarce and the agent can not find a place on the island suitable to sustain it with both trees and farming products simultaneously and, therefore, perishes quickly. Another issue is the unabated exponential growth of the population independent of population density. The model would greatly benefit from a smarter, more dynamic integration of the demography model by Puleston et al. (2017) and, in general, a more elaborate relation between the tree cutting, farming and population growth.

#### 4.2.4 Tree Preference

The change of the tree preference in response to local deforestation is the only far-sighted adaptation mechanism of the agents in the harvest process in response to environmental degradation. In the standard run configuration, an agent's tree preference responds linearly to the removal of trees. In Section 3.3, I presented three alternative adaptation strategies: Delayed, faster (i.e. with foresight), and logistic adaptation (first delayed, then faster) (see Figure 3.4). The mean tree preference of all agents,  $\bar{T}_{\text{Pref}, i}(t)$ , is shown in Figure 4.9 for ensembles of 15 realisations. The corresponding population dynamics is shown in Figure 4.10. The population size in the fast adaptation scenario peaks at a high value (and later) than in the other cases. The logistic formulation produces population dynamics that first resemble the case with delayed adaptation and later converges to the case with (standard) linear adaptation. By 1900 A.D., the population size is nearly twice as high for a fast vs. a delayed adapting society. Similarly, the dynamics of deforestation (Figure B.4) and of burnt trees (Figure B.5) depend on the tree preference adaptation strategy. E.g. while in the case with fast adaptation of the tree preference, the amount of burnt trees increases continuously from beginning to peak, especially in

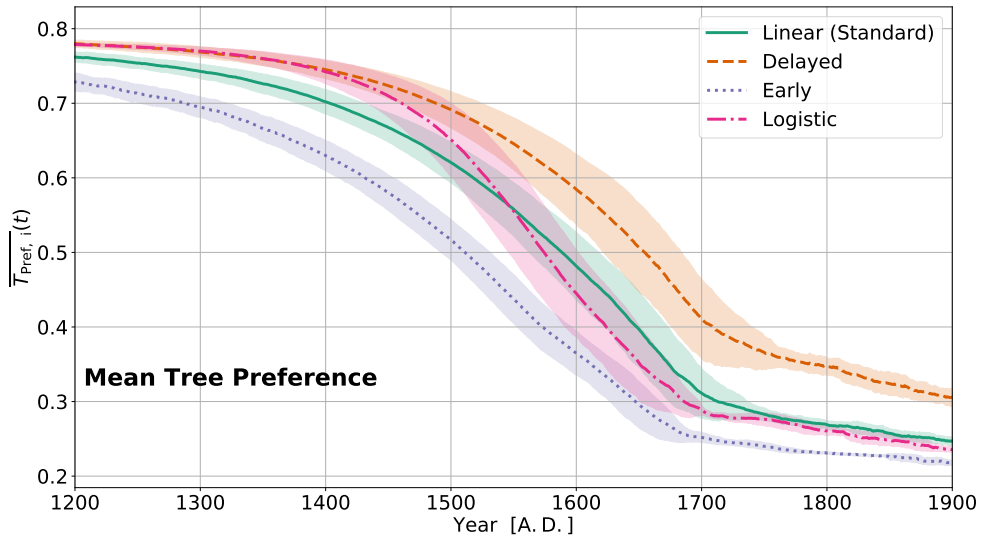


Figure 4.9: Mean tree preferences of all agents  $\overline{T}_{\text{Pref},i}(t)$  over time from an ensemble of each 15 different model realisations with different strategies to adapt the tree preference to the changing local tree density: Linear (standard setting), delayed, faster, or logistic (all shown in Figure 3.4).

the case with delayed and logistic adaptation, it remains constant (or even decreases) between 1300 and 1500 A.D. followed by a sharp increase afterwards. The summed amount of burnt trees is largest in the case with fast adaptation ( $5.3 \cdot 10^6$ ), compared to cases with linear ( $4.3 \cdot 10^6$ ), logistic ( $4.4 \cdot 10^6$ ) and delayed ( $3.3 \cdot 10^6$ ) adaptation. Counter-intuitively, more trees remain at the end of the simulations in the case with fast adaptation. The mean happiness of all agents is also slightly higher (or equivalent) for the fast adaptation strategy throughout the time period (not shown). In summary, the specific shape of the adaptation of the tree preference to the local environmental change has a non-trivial influence on the aggregate dynamics.

The results show that a fast (and early) adaptation of the tree preference seems to be the best strategy for the agents, maximising the peak and final population size, the amount of trees, and the mean happiness. While the logistic and linear strategies are quite similar in their aggregate outcomes, the peak population size is smaller for the logistic strategy. Hence, it seems that a better strategy for a civilisation in this model is to adapt linearly already during the early phase of local tree density change rather than to adapt only slowly and compensating this with a faster pace in the later phase (as in the logistic case).

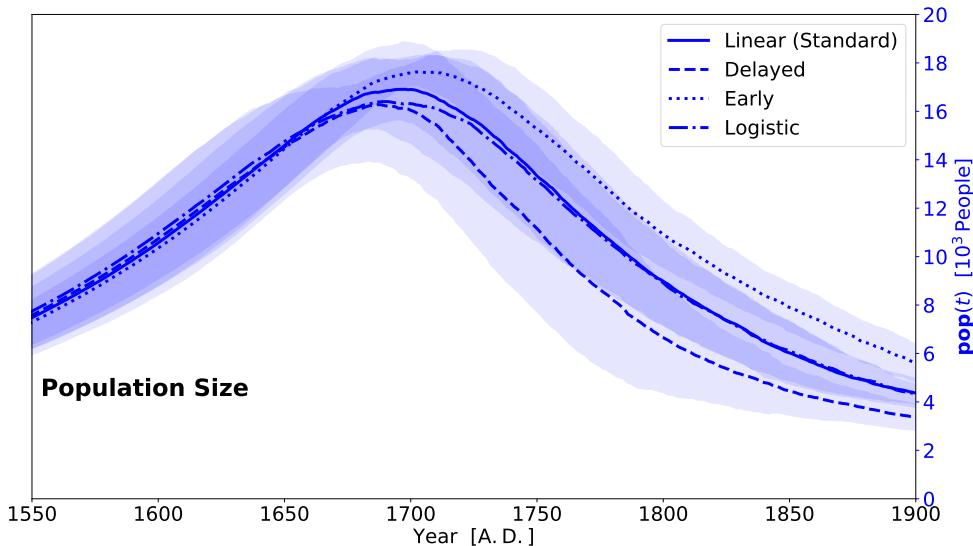


Figure 4.10: Total aggregate population dynamics for different adaptation strategies in relation to tree preference.

### 4.2.5 Moving Strategy

**Spatial and Aggregate Dynamics.** In the analysis so far, I have distinguished between spatial patterns and aggregate temporal dynamics. However, the results show that the spatial patterns also have an influence on the aggregate variables, population size, number of trees and number of burnt trees. Here, I investigate how three different decision making strategies in moving (see also Table 3.2) compare with the standard run. The strategies consider

- all penalties equally high, including some stochasticity (the standard run, as described in Figure 4.1)
- ‘only resource’ penalties (Figure 4.11), i.e.  $\alpha_T = \alpha_F = 0.5$  and all other weights are zero. With this strategy, agents spread out to all locations with access to arable, well-suited land irrespective of distance from freshwater, elevation, slope and population density. Consequently, the amount of trees burnt is larger in the period from 1200 to 1600 A.D. as there are no dense population centres in which collective tree cutting contributes to the clearing of land. Population peaks at a slightly later time and at a higher level. The following population size decrease after the peak is steeper and less individuals remain in 1900 A.D..
- only the ‘optimal location’ with the smallest penalty, i.e. a fully deterministic moving decision with  $\gamma \gg 1$  and  $\vec{\alpha}$  as in the standard run

configuration (Figure 4.12). Interestingly, agents cluster around ‘highly evaluated’ spots leading to a patchy spatial pattern. The aggregated population size (including the peak level), number of burnt trees or tree number are mostly unaffected by this, in comparison to the standard run but the variation in peak population size is smaller.

- no penalties or evaluation criteria at all, i.e. agents ignore all penalties ( $\gamma = 0$ ) and perform a ‘Trial&Error Hopping’ (Figure 4.13). Hence, an agent might ‘hop’ around in consecutive years until a spot with sufficient resource access is found, but burn trees to set up farms in all intermediate locations. This process delays the population growth, and, consequently, the population size peaks a century later (shortly before 1800 A.D.) but at a similar peak size compared to the standard run. The peak is followed by a rapid decline (up to 2% per year) to a third of the population size within less than a century.

The four different moving strategies presented here (Standard, Only Resources, Optimal Location and Trial&Error Hopping) do not only change the spatial pattern but also influence the overall dynamics of the model and, therefore, can not be simply ignored in the calculation of aggregate variables. This is especially apparent for the number of burnt trees. In particular, if agents do not move according to considerations (‘Trial&Error Hopping’ strategy), the overall population dynamics are affected, e.g. the decrease after the population size peak becomes steeper.

There is, of course, substantial freedom in modelling the evaluations of potential new locations and the decision making process related to moving. The framework is therefore kept flexible and other assumptions or new categories can easily be added or adjusted. There has not been any comparable approach for Easter Island society yet. In the ABM simulating the Anasazi people by Axtell et al. (2002) and Janssen (2009), agents that relocate their farms (and settlements) consider all eligible cells that fulfil certain nutrient production and water availability criteria and then choose the cell closest to the previous location. In general, I use a similar rationale but implement a more elaborate evaluation process that in particular introduces non-linear, continuous rather than binary evaluation criteria, more/different penalty categories and stochasticity in the decision making process. As shown, this procedure (in the standard run configuration) yields moving patterns that are consistent with plausible reconstructions on Easter Island history.

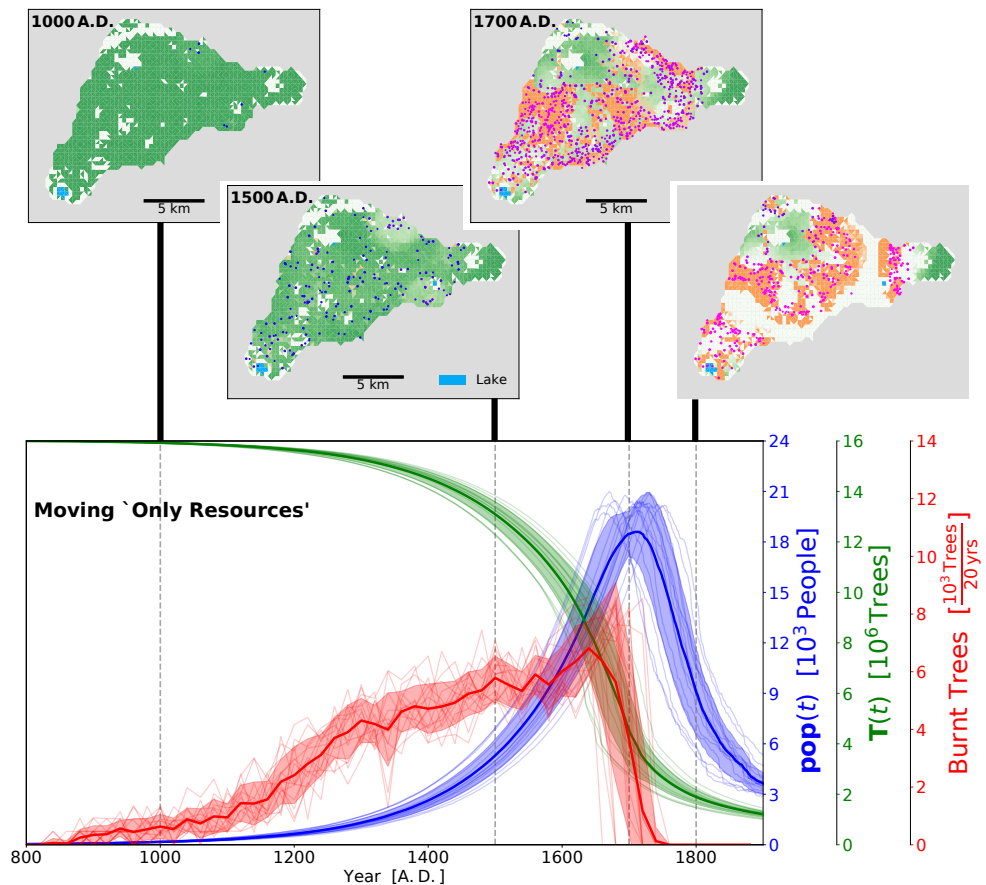


Figure 4.11: Moving strategy 'Only Resources'.

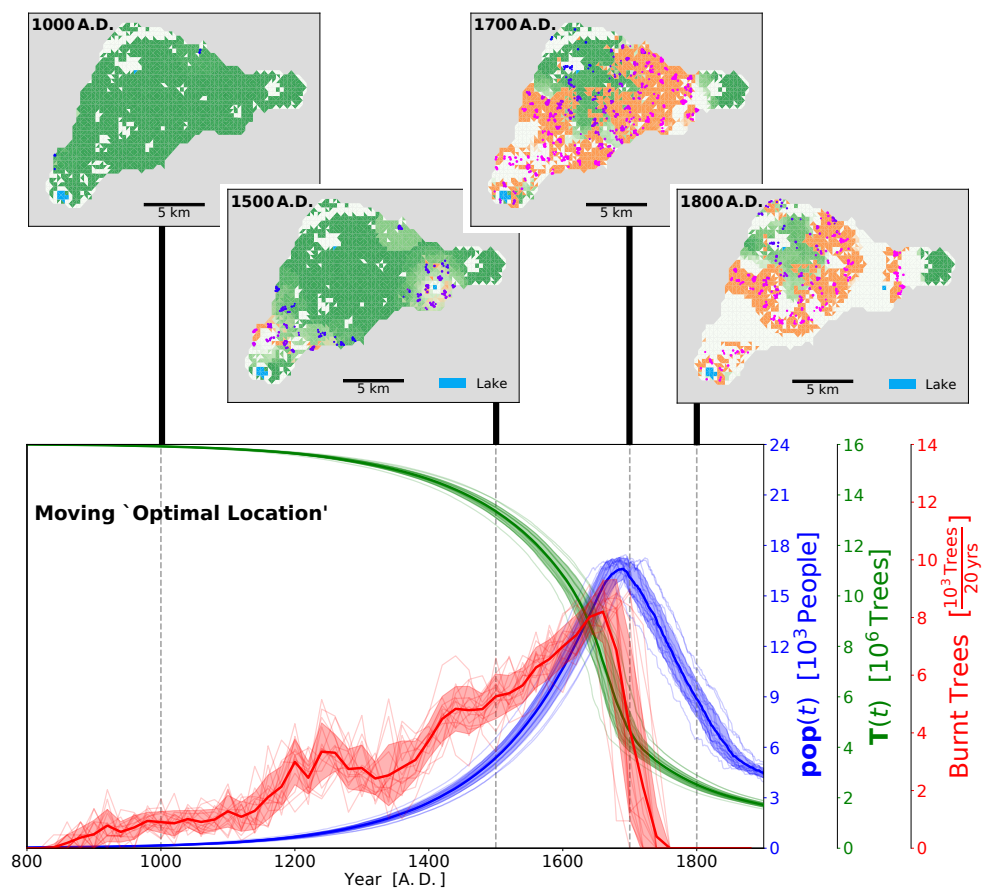


Figure 4.12: Moving strategy ‘Optimal Location’.

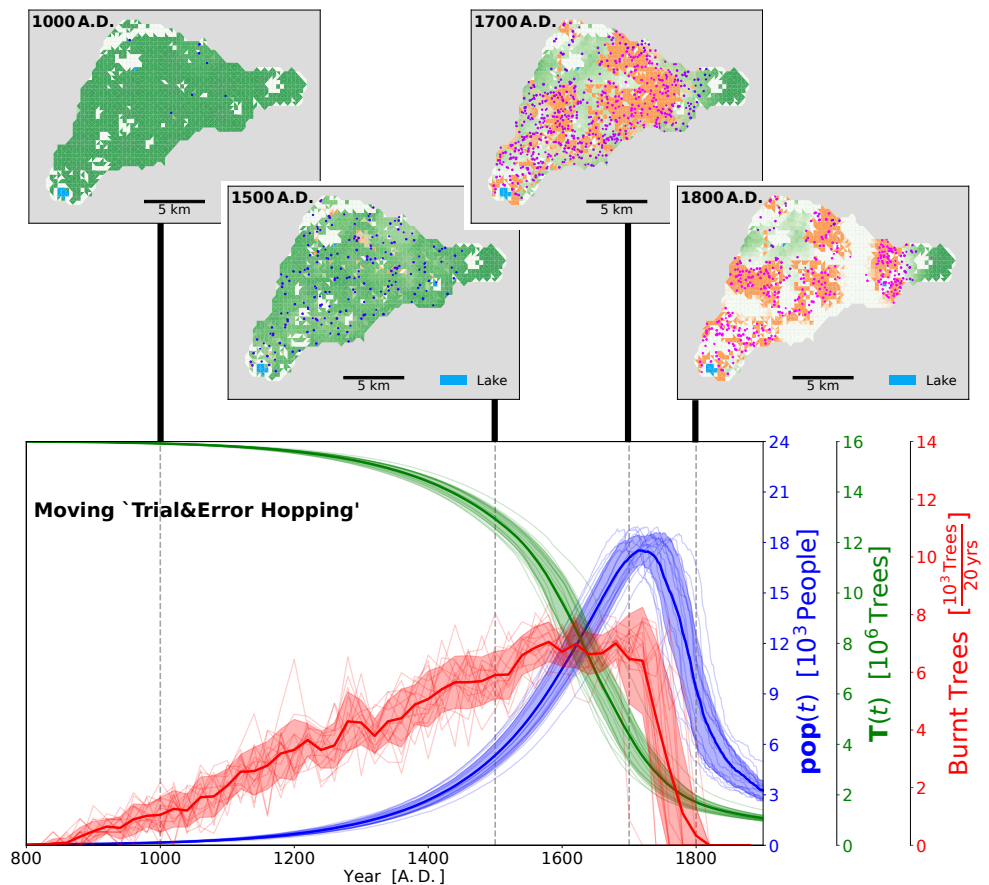


Figure 4.13: Moving strategy 'Trial&amp;Error Hopping'.

# **Chapter 5**

## **Conclusions**

Many studies on human-resource interaction in general and in relation to Easter Island history in particular have emphasized the importance of heterogeneous, spatial and stochastic considerations and the consequent constraints associated to modelling societies. E.g. Bousquet and Le Page (2004) describe the importance of modelling spatial and discrete characteristics, Merico (2017) points out gaps of Easter Island modelling with respect to these aspects, Rull (2020) argues that the spatio-temporal dynamics on Easter Island is heterogeneous, and Stevenson et al. (2015) among many other studies argues against an island-wide homogeneous dynamics before European contact. However, surprisingly very little effort has been put into quantifying such qualitative assessments. Here, I provided a first approach of a spatially explicit and realistic, stochastic and discrete model in the form of an Agent Based Model of human-resource interaction on Easter Island prior to European contact. The model simulates the settling of household agents interacting with a spatially explicit local environment.

The standard configuration run of the ABM presented here shows a boom and bust dynamics, i.e. an exponential growth of the population size, a short phase of peak population and a decrease (with the declining rate in the order of the initial growth rate) thereafter. This corresponds to the classical ecocidal narrative of Easter Island history sustained by Brander and Taylor (1998), Diamond (2011) and Bahn and Flenley (2017). Results that are more consistent with alternative population dynamic narratives, however, can be obtained by changing only a few parameters, in particular the tree regrowth and agricultural quality of the soil on Easter Island.

Despite several novel aspects, the model is based on a number of simplifications. First, there are numerous parameters describing both the environment

and the agent behaviour, which are subject to uncertainties and sometimes even chosen based on pure common sense due to lack of observational data. Agents in the model act entirely myopic (e.g. in the clearing of space for farming), self-centred and their harvest behaviour simply aims to maximise population size growth in each year regardless of future considerations or sustainability aspects. All agents have homogeneous conditions (e.g. the same penalty evaluation, tree preference adaptation strategy or minimum tree preference). There is neither agent-agent interaction, cooperation, trade nor any advanced economic or social structure (such as taboos). Further relevant simplifications are related to the population growth depending on resource harvest for a single agent, the oversimplified erosion process and the assumption of constant yields from farming sites regardless of e.g. labour considerations or climatic variation.

Despite these simplifications, the agent behaviour can be sufficiently well constructed through plausible, intuitive anthropogenic rules. As Kohler and Gumerman (2000) put it: "Agent construction at this point is more art than science". The impacts of some of the other simplifications are explored by testing different experiments and sensitivity of parameters.

By experimenting with different model configurations, this study provides three major results: First, the population decrease in the standard configuration run is caused by the lack of either farming sites or trees in all potential locations on Easter Island but not an island-wide lack of either of these resources. Second, the model shows how spatial considerations of microscopic units constrain the population dynamics overall and thus are computationally irreducible. E.g. varying the resource search radii or having different moving strategies impact the total number of burnt trees, deforestation, and population size. Third, slightly different strategies to adapt to environmental degradation lead to different outcomes overall in the model. More specifically, the best strategy is to quickly decrease the tree preference, i.e. the dependence on a non-renewable resource. While this fast transition leads to more trees being burnt to clear land, the population size throughout the time period and even the total number of trees are larger.

This ABM provides, for the first time, quantitative regional variations in the dynamics of population, trees, and agriculture, which are in many aspects consistent with qualitative descriptions in the literature (the ecocidal narrative). The regional dynamics are found to be very heterogeneous in shape and timing and far from a uniform island wide collapse. Such spatio-temporal patterns emerge from the assumption of discrete, non-ergodic, stochastic and individual decision making processes of the agents. An important implication of these

results is that archaeological data obtained in single sites cannot be directly extrapolated to explain island-wide population dynamics. In general, the model gives a novel view on Easter Island by adding relevant spatial considerations to the ongoing debate about the island's history before European contact.

A major advantage of Agent Based Modelling is its flexibility and the fact that the complexity of the model does not need to be fixed *a priori* (Bonabeau, 2002). The presented model can easily incorporate more, different or less modules, rules or processes. Model development including the emergence of social institutions as suggested in the Discussion, is an obvious avenue for future research with the potential to further improve our understanding of the history of Easter Island before European contact and, thereby, to explore the general concept of overpopulation in a world with limited resources.

# Bibliography

- Axtell, R. L. et al. (2002). “Population growth and collapse in a multiagent model of the Kayenta Anasazi in Long House Valley”. In: *Proceedings of the National Academy of Sciences of the United States of America*. ISSN: 00278424. doi: 10.1073/pnas.092080799.
- Bahn, P. and J. Flenley (2017). *Easter Island, Earth Island: The enigmas of Rapa Nui*. 4th ed. Maryland, USA: Rowman & Littlefield. ISBN: 9781442266551.
- Basener, W. et al. (2008). “Rat instigated human population collapse on Easter Island”. In: *Nonlinear Dynamics, Psychology, and Life Sciences*. ISSN: 10900578.
- Basener, W. et al. (2011). “Spatial effects and Turing instabilities in the invasive species model”. In: *Nonlinear Dynamics, Psychology, and Life Sciences*. ISSN: 10900578.
- Bengfort, B. et al. (Nov. 14, 2018). *Yellowbrick*. Version 0.9.1. doi: 10.5281/zenodo.1206264. URL: <http://www.scikit-yb.org/en/latest/>.
- Bonabeau, E. (2002). “Agent-based modeling: Methods and techniques for simulating human systems”. In: *Proceedings of the National Academy of Sciences of the United States of America*. ISSN: 00278424. doi: 10.1073/pnas.082080899.
- Bookstaber, R. (2019). *The end of theory: Financial crises, the failure of economics, and the sweep of human interaction*. Princeton University Press.
- Bousquet, F. and C. Le Page (2004). “Multi-agent simulations and ecosystem management: A review”. In: *Ecological Modelling*. ISSN: 03043800. doi: 10.1016/j.ecolmodel.2004.01.011.
- Brander, J. A. and M. S. Taylor (1998). “The Simple Economics of Easter Island: A Ricardo-Malthus Model of Renewable Resource Use”. In: *American Economic Review*. ISSN: 00028282. doi: 10.2307/116821.
- Brandt, G. and A. Merico (2015). “The slow demise of Easter Island: Insights from a modeling investigation”. In: *Frontiers in Ecology and Evolution*. ISSN: 2296701X. doi: 10.3389/fenvo.2015.00013.

- Bungartz, H.-J. et al. (2009). *Modellbildung und Simulation: Eine anwendungssorientierte Einführung*. ISBN: 9783540798095. doi: 10.1007/978-3-540-79810-1.
- Cauwe, N. and N. Latsanopoulos (2011). *Easter Island : the great taboo : rebuilding its history after ten years of excavations*. Versant Sud Louvain-la-Neuve, Belgium, p. 157. ISBN: 2930358556. URL: <https://nla.gov.au/nla.cat-vn5753756>.
- Cole, A. and J. Flenley (2008). “Modelling human population change on Easter Island far-from-equilibrium”. In: *Quaternary International*. ISSN: 10406182. doi: 10.1016/j.quaint.2007.09.019.
- D’Alessandro, S. (2007). “Non-linear dynamics of population and natural resources: The emergence of different patterns of development”. In: *Ecological Economics*. ISSN: 09218009. doi: 10.1016/j.ecolecon.2006.07.008.
- Diamond, J. (2011). *Collapse: How Societies Choose to Fail or Succeed: Revised Edition*. Penguin Publishing Group. ISBN: 9781101502006. URL: <https://books.google.de/books?id=mYPXUHZCp3gC>.
- Good, D. H. and R. Reuveny (2006). “The fate of Easter Island: The limits of resource management institutions”. In: *Ecological Economics*. ISSN: 09218009. doi: 10.1016/j.ecolecon.2005.07.022.
- Gorelick, N. et al. (2017). “Google Earth Engine: Planetary-scale geospatial analysis for everyone”. In: *Remote Sensing of Environment*. doi: 10.1016/j.rse.2017.06.031. URL: <https://doi.org/10.1016/j.rse.2017.06.031>.
- Heckbert, S. (2013). “MayaSim: An agent-based model of the ancient Maya social-ecological system”. In: *JASSS*. ISSN: 14607425. doi: 10.18564/jasss.2305.
- Hunt, T. L. (2007). “Rethinking Easter Island’s ecological catastrophe”. In: *Journal of Archaeological Science*. ISSN: 03054403. doi: 10.1016/j.jas.2006.10.003.
- Hunter, J. D. (2007). “Matplotlib: A 2D graphics environment”. In: *Computing in Science & Engineering* 9.3, pp. 90–95. doi: 10.1109/MCSE.2007.55.
- Janssen, M. A. (2009). “Understanding Artificial Anasazi”. In: *JASSS*. ISSN: 14607425.
- Jarvis, A. et al. (2008). *Hole-filled SRTM for the globe Version 4*. available from the CGIAR-CSI SRTM 90m Database: <http://srtm.csi.cgiar.org>.

- KC, S. and W. Lutz (2017). “The human core of the shared socioeconomic pathways: Population scenarios by age, sex and level of education for all countries to 2100”. In: *Global Environmental Change*. ISSN: 09593780. doi: 10.1016/j.gloenvcha.2014.06.004.
- Kirch, P. V. (2010). *How chiefs became kings: Divine kingship and the rise of archaic states in ancient Hawai'i*. ISBN: 9780520267251. doi: 10.5860/choice.49-0954.
- Kohler, T. A. and G. G. Gumerman (2000). *Dynamics in human and primate societies: Agent-based modeling of social and spatial processes*. Oxford University Press.
- Lee, C. T. and S. Tuljapurkar (2008). *Population and prehistory I: Food-dependent population growth in constant environments*. doi: 10.1016/j.tpb.2008.03.001.
- Louwagie, G., C. M. Stevenson, and R. Langohr (2006). “The impact of moderate to marginal land suitability on prehistoric agricultural production and models of adaptive strategies for Easter Island (Rapa Nui, Chile)”. In: *Journal of Anthropological Archaeology*. ISSN: 02784165. doi: 10.1016/j.jaa.2005.11.008.
- Malthus, T. R. (1798). “An essay on the principle of population as it affects the future improvement of society, with remarks on the speculations of Mr Godwin, M”. In: *Condorcet, and other writers*. London: J. Johnson.
- Meadows, D. H. et al. (1972). “The limits to growth”. In: *New York* 102, p. 27.
- Merico, A. (2017). *Models of easter island human-resource dynamics: Advances and gaps*. doi: 10.3389/fenv.2017.00154.
- Mieth, A and H. Bork (2015). “Degradation of resources and successful land-use management on prehistoric Rapa Nui: Two sides of the same coin”. In: *Easter Island: Collapse or Transformation*, pp. 9–10.
- Mieth, A. and H. R. Bork (2005). “History, origin and extent of soil erosion on Easter Island (Rapa Nui)”. In: *Catena*. doi: 10.1016/j.catena.2005.06.011.
- Müller-Hansen, F. et al. (2017). “Towards representing human behavior and decision making in Earth system models - An overview of techniques and approaches”. In: *Earth System Dynamics* 8.4, pp. 977–1007. ISSN: 21904987. doi: 10.5194/esd-8-977-2017.
- Oliphant, T. E. (2006). *A guide to NumPy*. Vol. 1. Trelgol Publishing USA.
- Pedregosa, F. et al. (2011). “Scikit-learn: Machine Learning in Python”. In: *Journal of Machine Learning Research* 12, pp. 2825–2830.
- Puleston, C. O. and S. Tuljapurkar (2008). “Population and prehistory II: Space-limited human populations in constant environments”. In: *Theoretical Pop-*

- ulation Biology*. ISSN: 00405809. doi: 10.1016/j.tpb.2008.05.007.
- Puleston, C. O. et al. (2017). “Rain, sun, soil, and sweat: A consideration of population limits on Rapa Nui (Easter Island) before European contact”. In: *Frontiers in Ecology and Evolution*. ISSN: 2296701X. doi: 10.3389/fevo.2017.00069.
- Reuveny, R. (2012). “Taking Stock of Malthus: Modeling the Collapse of Historical Civilizations”. In: *Annual Review of Resource Economics*. ISSN: 1941-1340. doi: 10.1146/annurev-resource-110811-114537.
- Rull, V. et al. (2010). *Paleoecology of Easter Island: Evidence and uncertainties*. doi: 10.1016/j.earscirev.2010.02.003.
- Rull, V. (2020). “The deforestation of Easter Island”. In: *Biological Reviews*. ISSN: 1469185X. doi: 10.1111/brv.12556.
- Rull, V. et al. (2016). *Three millennia of climatic, ecological, and cultural change on Easter Island: An integrative overview*. doi: 10.3389/fevo.2016.00029.
- Stevenson, C. M. et al. (2015). “Variation in Rapa Nui (Easter Island) land use indicates production and population peaks prior to European contact”. In: *Proceedings of the National Academy of Sciences of the United States of America*. ISSN: 10916490. doi: 10.1073/pnas.1420712112.
- Virtanen, P. et al. (2020). “SciPy 1.0: Fundamental Algorithms for Scientific Computing in Python”. In: *Nature Methods* 17, pp. 261–272. doi: <https://doi.org/10.1038/s41592-019-0686-2>.

# Appendix A

## More Details of the Model

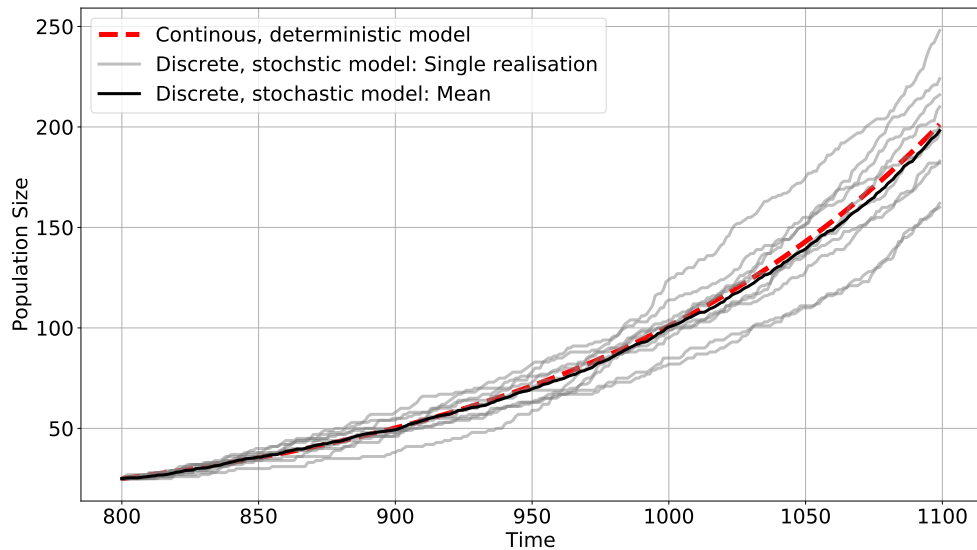


Figure A.1: Realisations (and the mean) of the discrete, stochastic population growth model (assuming  $H_i(t) = 1$  for all  $t$  here. In comparison, the continuous exponential growth. The growth rate is  $g(H_i(t) = 1) = 1.007$ , as in the standard setting of the model.

# Appendix B

## More Results

### B.1 Additional Results: Standard Run

On [https://github.com/PeterSteiglechner/Masterthesis\\_ZMT\\_2020](https://github.com/PeterSteiglechner/Masterthesis_ZMT_2020), I provide an animated figure showing the spatial pattern of Easter Island settlement, deforestation and agricultural production in one single realisation of the standard run over time.

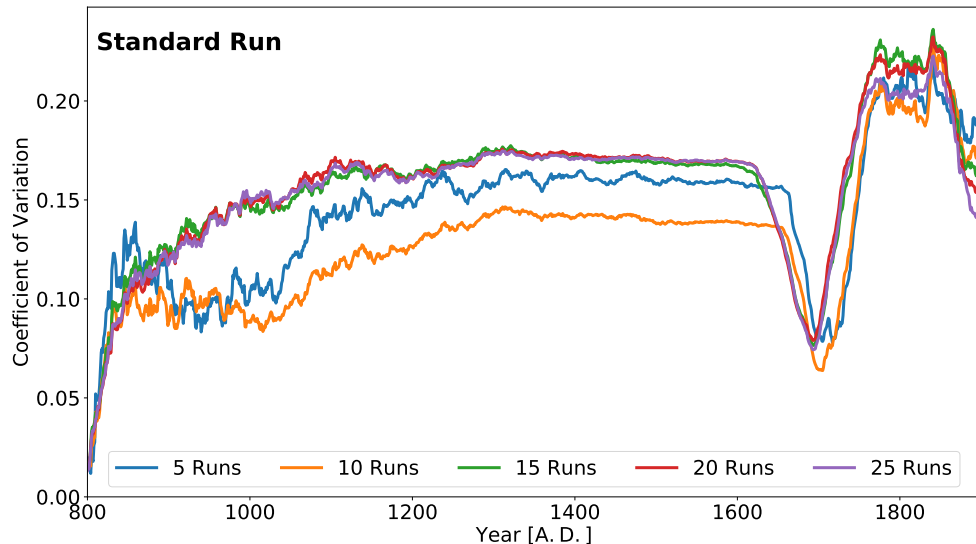


Figure B.1: The coefficient of variation of ensembles of 5 to 25 runs for the Standard run over time. For more than 15 runs, the coefficient of variation does not change significantly and, thus, this provides a good ensemble size

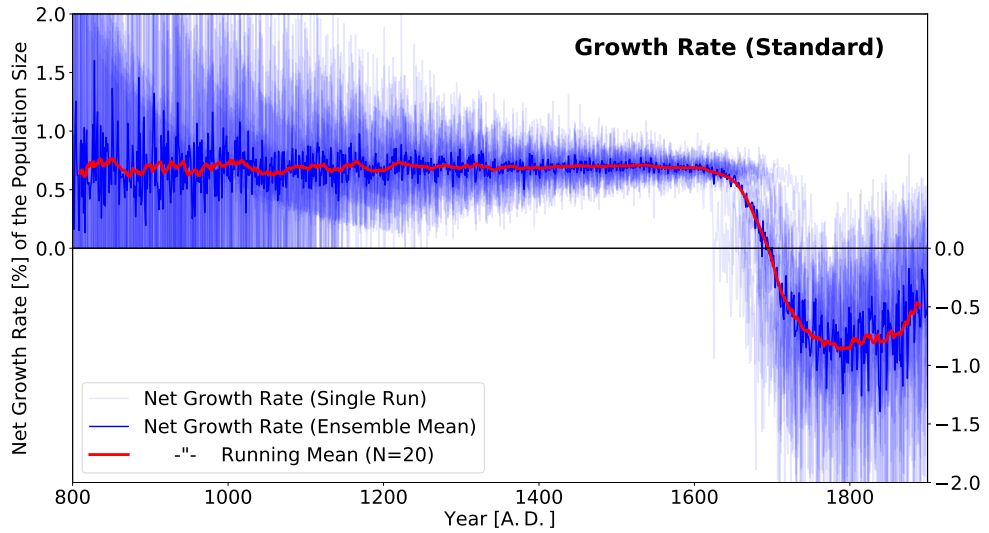


Figure B.2: Ensemble of five Standard runs. The net population growth rate is shown as the mean of the ensemble (blue) and, for easier visibility, as a running mean (red).

## B.2 Clustering the Agents

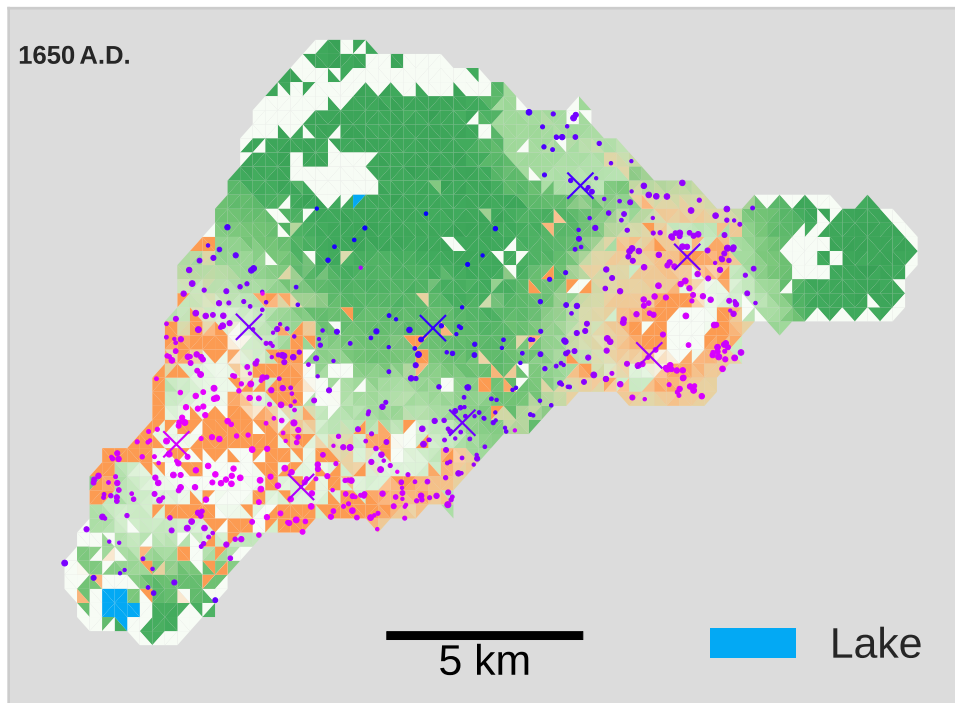


Figure B.3: The map shows one realisation of the Standard run. The agents are assigned to clusters with midpoints (crosses) by a k-Means algorithm of the three dimensional state vectors  $(x_i, y_i, T_{\text{Pref}, i}) (t)$  for agent  $i$  in the year 1650 A.D..

### B.3 Additional Results: Variation in the Agents' Strategy of Adapting the Tree Preference

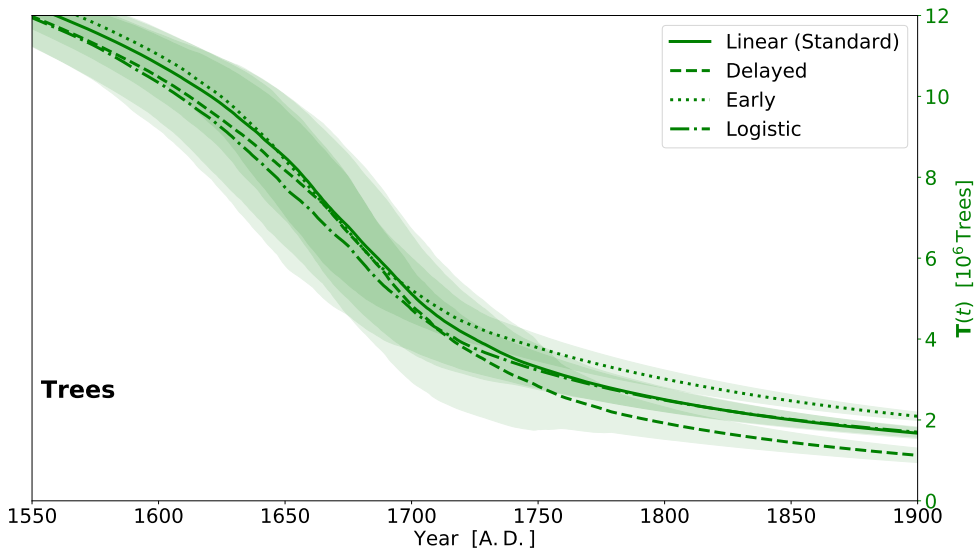


Figure B.4: Number of Burnt Trees in the four different Adoption strategies of the tree preference.

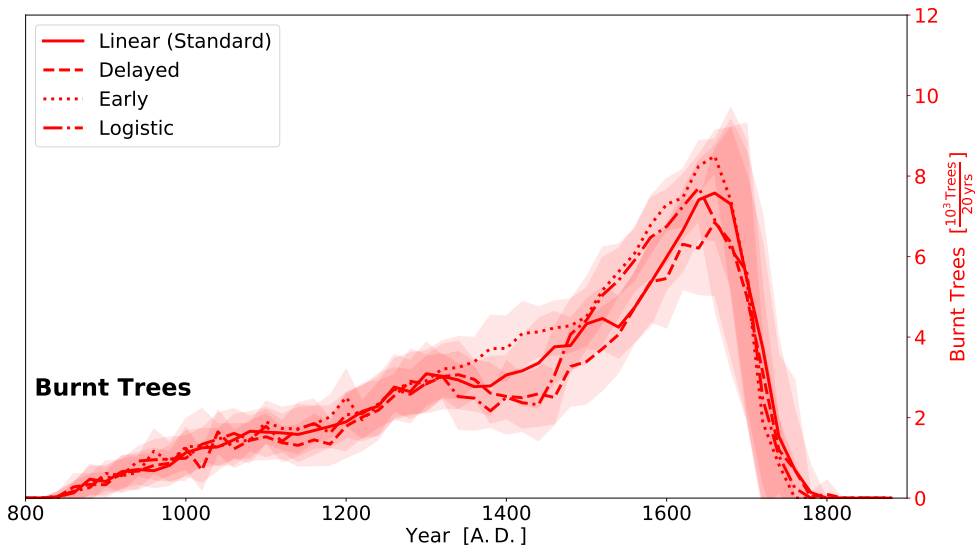


Figure B.5: Number of Burnt Trees in the four different Adoption strategies of the tree preference.



